
INTERPRETABILITY IS IN THE MIND OF THE BEHOLDER: A CAUSAL FRAMEWORK FOR HUMAN-INTERPRETABLE REPRESENTATION LEARNING

A PREPRINT

Emanuele Marconato
DISI, University of Trento, Italy
DI, University of Pisa, Italy
emanuele.marconato@unitn.it

Andrea Passerini
DISI, University of Trento, Italy
andrea.passerini@unitn.it

Stefano Teso
CIMeC and DISI, University of Trento, Italy
stefano.teso@unitn.it

September 10, 2023

ABSTRACT

Focus in Explainable AI is shifting from explanations defined in terms of low-level elements, such as input features, to explanations encoded in terms of *interpretable concepts learned from data*. How to reliably acquire such concepts is, however, still fundamentally unclear. An agreed-upon notion of concept interpretability is missing, with the result that concepts used by both *post-hoc* explainers and *concept-based* neural networks are acquired through a variety of mutually incompatible strategies. Critically, most of these neglect the human side of the problem: *a representation is understandable only insofar as it can be understood by the human at the receiving end*. The key challenge in Human-interpretable Representation Learning (HRL) is how to model and operationalize this human element. In this work, we propose a mathematical framework for acquiring *interpretable representations* suitable for both post-hoc explainers and concept-based neural networks. Our formalization of HRL builds on recent advances in causal representation learning and explicitly models a human stakeholder as an external observer. This allows us derive a principled notion of *alignment* between the machine’s representation and the vocabulary of concepts understood by the human. In doing so, we link alignment and interpretability through a simple and intuitive *name transfer* game, and clarify the relationship between alignment and a well-known property of representations, namely *disentanglement*. We also show that alignment is linked to the issue of undesirable correlations among concepts, also known as *concept leakage*, and to content-style separation, all through a general information-theoretic reformulation of these properties. Our conceptualization aims to bridge the gap between the human and algorithmic sides of interpretability and establish a stepping stone for new research on human-interpretable representations.

Keywords explainable AI · causal representation learning · alignment · disentanglement · causal abstractions · concept leakage

1 Introduction

The field of Explainable AI (XAI) has developed a wealth of attribution techniques for unearthing the reasons behind the decisions of black-box machine learning models [Guidotti et al., 2018]. Tradition-

ally, explaining a prediction involves identifying and presenting those low-level *atomic elements* – like input variables [Štrumbelj and Kononenko, 2014, Ribeiro et al., 2016] and training examples [Kim et al., 2016, Koh and Liang, 2017] – that are responsible for said prediction. Explanations output by white-box models, such as sparse linear classifiers [Ustun and Rudin, 2016] and rule-based predictors [Wang et al., 2017], follow the same general setup. These atomic elements, however, are not very expressive and, as such, can be ambiguous [Rudin, 2019]. To see this, consider an image of a red sports car that is tagged as “positive” by a black-box predictor. In this example, a saliency map would highlight those *pixels* that are most responsible for this prediction: these do not say whether the prediction depends on the image containing a “car”, on the car being “red”, or on the car being “sporty”. As a consequence, it is impossible to understand what the model is “thinking” and how it would behave on other images based on this explanation alone [Teso et al., 2023].

This is why focus in XAI has recently shifted toward explanations expressed in terms of higher-level symbolic representations, or *concepts* for short. These promise to ensure explanations are rich enough they can capture the machine’s reasoning patterns, while being expressed in terms that can be naturally understood by stakeholders [Rudin, 2019, Kambhampati et al., 2022].

This trend initially emerged with (*post-hoc*) *concept-based explainers* (CBEs) like TCAV [Kim et al., 2018] and Net2Vec [Fong and Vedaldi, 2018], among others [Ghorbani et al., 2019, Zhang et al., 2021, Fel et al., 2023a], which match the latent space of a deep neural network to a vocabulary of pre-trained concept detectors.¹ These were quickly followed by a variety of *concept-based models* (CBMs) – including Self-Explainable Neural Networks [Alvarez-Melis and Jaakkola, 2018], Part-Prototype Networks [Chen et al., 2019], Concept-Bottleneck Models [Koh et al., 2020], GlanceNets [Marconato et al., 2022], and Concept Embedding Models [Espinosa Zarlenga et al., 2022] – that support representation learning while retaining interpretability. Specifically, these approaches learn a neural mapping from inputs to concepts, and then leverage the latter for both computing predictions – in a simulatable manner [Lipton, 2018] – and providing *ante-hoc* explanations thereof. See [Schwalbe, 2022] for a review. Since concepts act as a *bottleneck* through which all information necessary for inference must flow, CBMs hold the promise of avoiding the lack of faithfulness typical of post-hoc techniques, while enabling a number of useful operations such as interventions [Koh et al., 2020] and debugging [Stammer et al., 2021, Bontempelli et al., 2023] using concepts as a human-friendly interface.

1.1 Limitations of Existing Works

The promise of conceptual explanations rests on the assumption that learned concepts are themselves interpretable. This begs the question: *what does it mean for a vocabulary of concepts to be interpretable?*

Researchers have proposed a variety of practical strategies to encourage the interpretability of the learned concepts, but no consistent recipe. Some CBMs constrain their representations according to intuitive heuristics, such as similarity to concrete training examples [Chen et al., 2019] or activation sparsity [Alvarez-Melis and Jaakkola, 2018]. However, the relationship between these properties and interpretability is unclear, and unsurprisingly there are well known cases in which CBMs acquire concepts activating on parts of the input with no obvious semantics [Hoffmann et al., 2021, Xu-Darme et al., 2023]. A more direct way of controlling the semantics of learned concepts is to leverage *supervision* on the concepts themselves, a strategy employed by both CBEs [Kim et al., 2018] and CBMs [Koh et al., 2020, Chen et al., 2020, Marconato et al., 2022]. Unfortunately, this is no panacea, as doing so cannot prevent *concept leakage* [Margeloiu et al., 2021, Mahinpei et al., 2021], whereby information from a concept “leaks” into another, seemingly unrelated concept, compromising its meaning.

At the same time, concept quality is either assessed qualitatively in a rather unsystematic fashion – *e.g.*, by inspecting the concept activations or saliency maps on a handful of examples – or quantitatively, most often by measuring how well learned concepts match annotations. This so-called *concept accuracy*, however, is insufficient to capture issues like concept leakage.

Besides these complications, existing approaches neglect a critical aspect of this learning problem: that *interpretability is inherently subjective*. For instance, explaining a prediction to a medical doctor requires different concepts than explaining it to a patient: the notion of “intraepithelial” may be essential for the former, while being complete gibberish to the latter. However, even when concept annotations are employed, they are gathered from offline repositories and as such they may not capture concepts that are

¹The idea of using higher-level concepts was foreshadowed in the original LIME paper [Ribeiro et al., 2016].

meaningful to a particular expert, or that despite being associated with a familiar name follow semantics incompatible with those the user attaches to that name.²

1.2 Our Contributions

Motivated by these observations, we propose to view interpretability as the machine’s ability to communicate with a specific human-in-the-loop. Specifically, we are concerned with the problem of learning conceptual representations that enable this kind of communication for both *post-* and *ante-hoc* explanations. We call this problem **human-interpretable representation learning**, or HRL for short. Successful communication is essential for ensuring human stakeholders can understand *explanations* based on the learned concepts and, in turn, realizing the potential of CBEs and CBMs. This view is compatible with recent interpretations of the role of symbols in neuro-symbolic AI [Silver and Mitchell, 2023, Kambhampati et al., 2022]. The key question is how to model this human element in a way that can be actually *operationalized*. We aim to fill this gap.

Our first contribution is a conceptual and mathematical model – resting on techniques from causal representation learning [Schölkopf et al., 2021] – of HRL that *explicitly models the human-in-the-loop*.

As a second contribution, we leverage our formalization to develop an intuitive but sound notion of *alignment* between the conceptual representation used by the machine and that of the human observer. Alignment is strictly related to *disentanglement*, a property of learned representations frequently linked to interpretability [Bengio et al., 2013, Higgins et al., 2018], but also strictly *stronger*, in the sense that disentanglement alone is insufficient to ensure concept interpretability. We propose that alignment is key for evaluating interpretability of both CBEs and CBMs.

Our formalization improves on the work of Marconato et al. [2022] and looks at three settings of increasing complexity and realism: (i) a simple but non-trivial setting in which the human’s concepts are *disentangled* (i.e., individual concepts can be changed independently from each other without interference). (ii) a more general setting in which the human’s concepts are constrained to be disentangled in blocks; (iii) an unrestricted setting in which the human concepts can influence each other in arbitrary manners. In addition, we identify a and previously ignored link between interpretability of representations and the notion of *causal abstraction* [Beckers and Halpern, 2019, Beckers et al., 2020, Geiger et al., 2023a].

As a third contribution, we formally show that *concept leakage* can be viewed as a lack of disentanglement, and therefore of alignment. This strengthens existing results and allows to reinterpret previous empirical observations [Marconato et al., 2022, Lockhart et al., 2022].

As a fourth contribution, we discuss key questions arising from our mathematical framework, including whether perfect alignment is sufficient and necessary for interpretability, how to measure it, how to implement it in representation learning, and how to collect the necessary concept annotations.

1.3 Outline

The remainder of this paper is structured as follows. In the next section, we introduce prerequisite material and then proceed in section 3 to formalize the problem of human-interpretable representation learning and cast concept interpretability in terms of *alignment between representations*. Next, in section 4 we analyze in depth the notion of alignment in three settings of increasing complexity and study its relationship to the issue of concept leakage, and then look at the consequences of our formalization in section 5. Finally, we discuss related works in section 6 and offer some concluding remarks in section 7.

2 Preliminaries

In the following, we indicate scalar constants x in lower-case, random variables X in upper case, ordered sets of constants \mathbf{x} and random variables \mathbf{X} in bold typeface, and index sets \mathcal{I} in calligraphic typeface. We also use the shorthand $[n] := \{1, \dots, n\}$. Letting $\mathbf{X} = (X_1, \dots, X_n)$ and $\mathcal{I} \subseteq [n]$, we write $\mathbf{X}_{\mathcal{I}} := (X_i : i \in \mathcal{I})$ to indicate the ordered subset indexed by \mathcal{I} and $\mathbf{X}_{-\mathcal{I}} := \mathbf{X} \setminus \mathbf{X}_{\mathcal{I}}$ to denote its complement, and abbreviate $\mathbf{X} \setminus \{X_i\}$ as \mathbf{X}_{-i} .

²Of course, there are exceptions to this rule. These are discussed in section 6.



Figure 1: SCMs illustrating two different notions of disentanglement. *Left*: The variables $\mathbf{G} = \{G_1, \dots, G_n\}$ are disentangled. *Right*: Typical data generation and encoding process used in deep latent variable models. The machine representation $\mathbf{M} = \{M_1, \dots, M_k\}$ is *disentangled with respect to* the generative factors \mathbf{G} if and only if each M_j encodes information about at most one G_i .

2.1 Structural Causal Models and Interventions

A *structural causal model* (SCM) is a formal description of the causal relationships existing between parts of a (stochastic) system [Pearl, 2009, Peters et al., 2017]. Formally, an SCM \mathcal{C} specifies a set of *structural assignments* encoding direct causal relationships between variables,³ in the form:

$$X_i \leftarrow f_i(\mathbf{Pa}_i, N_i) \quad (1)$$

where $\mathbf{X} = (X_1, \dots, X_n)$ are variables encoding the state of the system, $\mathbf{Pa}_i \subseteq \mathbf{X}$ are the direct causes of X_i , and N_i are noise terms. Variables without parents are *exogenous*, and play the role of inputs to the system, while the others are *endogenous*. The full state of the system can be sampled by propagating the values of the exogenous variables through the structural assignments in a top-down fashion. SCMs can be viewed as *graphs* in which nodes represent variables, arrows represent assignments, and noise variables are usually suppressed, cf. fig. 1.

Following common practice, we assume the noise terms to be mutually independent from each other and also independent from the variables not appearing in the corresponding structural equations, that is, it holds that $N_i \perp\!\!\!\perp N_j$ for all $i \neq j$ and $N_i \perp\!\!\!\perp X_j$ for all i, j . This is equivalent to assuming there are no hidden confounders. This assumption carries over to all SCMs used throughout the paper.

An SCM \mathcal{C} describes both a *joint distribution* $p(\mathbf{X}) = \prod_i p(X_i \mid \mathbf{Pa}_i)$ and how this distribution *changes* upon performing *interventions* on the system. These are modifications to the system’s variables and connections performed by an external observer. Using Pearl’s *do*-operator [Pearl, 2009], (atomic) interventions can be written as $do(X_i \leftarrow x_i)$, meaning that the value of the variable X_i is forcibly changed to the value x_i , regardless of the state of its parents and children. Carrying out an atomic intervention yields a *manipulated SCM* identical to \mathcal{C} except that all assignments to X_i are deleted (*i.e.*, the corresponding links in the graph disappear) and all occurrences of X_i in the resulting SCM are replaced by the constant x_i . The resulting manipulated distribution is $p(\mathbf{X} \mid do(X_i \leftarrow x_i)) = \mathbb{1}\{X_i = x_i\} \cdot \prod_{j \neq i} p(X_j \mid \mathbf{Pa}_j)$. Non-atomic interventions of the form $do(\mathbf{X}_{\mathcal{I}} \leftarrow \mathbf{x}_{\mathcal{I}})$ work similarly. Expectations of the form $\mathbb{E}[\cdot \mid do(X_j \leftarrow x_j)]$ are just regular expectations evaluated with respect to the manipulated distribution.

2.2 Disentanglement

Central to our work is the notion of disentanglement [Higgins et al., 2018, Eastwood and Williams, 2018, Schölkopf et al., 2021] in both its two acceptations, namely *disentanglement of variables* and *disentanglement of representations*. We henceforth rely on the causal formalization given by Suter et al. [2019] and Reddy et al. [2022]. We refer the reader to those papers for more details.

Intuitively, a *set of variables* $\mathbf{G} = (G_1, \dots, G_n)$ is *disentangled* if the variables can be changed independently from one another. For instance, if G_1 represents the “color” of an object and G_2 its “shape”, disentanglement of variables implies that changing the object’s color does not impact its shape. This should hold even if the variables \mathbf{G} have a common set of parents \mathbf{C} – playing the role of counfounders,

³As customary, we work with SCMs that are *acyclic*, *causally sufficient* (*i.e.*, there are no external, hidden variables influencing the system), and *causally Markovian* (*i.e.*, each variable X_i is independent of its non-descendant given its parents in the SCM) [Pearl, 2009].

such as sampling bias or choice of source domain [Pearl, 2009] – meaning that they can be both disentangled *and* correlated (via \mathbf{C}). From a causal perspective, disentanglement of variables can be defined as follows:

Definition 1 (Disentanglement of variables) *A set of variables \mathbf{G} are disentangled if and only if $p(G_i | \mathbf{C}, do(\mathbf{G}_{\mathcal{I}} \leftarrow \mathbf{g}'_{\mathcal{I}})) \equiv p(G_i | \mathbf{C})$ for all possible choices of $\mathcal{I} \subseteq [n] \setminus \{i\}$ and $\mathbf{g}'_{\mathcal{I}}$.*

Now, consider the SCM in fig. 1 (left). It is easy to see that the variables \mathbf{G} are disentangled: any intervention $do(\mathbf{G}_{\mathcal{I}} \leftarrow \mathbf{g}'_{\mathcal{I}})$ breaks the links from \mathbf{C} to $\mathbf{G}_{\mathcal{I}}$, meaning that changes to the latter will not affect G_i . In this case, the variables \mathbf{G} are also conditionally independent from one another given \mathbf{C} , or equivalently $G_i \perp\!\!\!\perp G_j | \mathbf{C}$ for every $i \neq j$.

Later on, we will be concerned with data generation processes similar to the one illustrated in fig. 1 (right). Here, a set of *generative factors* $\mathbf{G} = (G_1, \dots, G_n)$ with common parents \mathbf{C} cause an observation \mathbf{X} , and the latter is encoded into a *representation* $\mathbf{M} = (M_1, \dots, M_k)$ by a machine learning model $p_{\theta}(\mathbf{M} | \mathbf{X})$. Specifically, \mathbf{M} is obtained by marginalizing over the inputs \mathbf{X} :

$$p_{\theta}(\mathbf{M} | \mathbf{G}) := \mathbb{E}_{\mathbf{x} \sim p(\mathbf{x} | \mathbf{G})} [p_{\theta}(\mathbf{M} | \mathbf{x})] \quad (2)$$

This can also be viewed as a *stochastic map* $\alpha : \mathbf{g} \mapsto \mathbf{m}$. Maps of this kind are central to our discussion.

Since \mathbf{G} is disentangled (cf. definition 1), we can talk about *disentanglement of representations* for \mathbf{M} . We say that \mathbf{M} is *disentangled with respect to \mathbf{G}* if, roughly speaking, each M_j encodes information about at most one G_i , or – more precisely – *as long as G_i is kept fixed, the value of M_j does not change even when the remaining factors $\mathbf{G} \setminus \{G_i\}$ are forcibly modified via interventions*. The degree by which a representation *violates* disentanglement of representations can be measured using the PIDA metric:

Definition 2 (PIDA [Suter et al., 2019]) *Let G_i be a generative factor and M_j an element of the machine representation. PIDA measures how much fixing G_i to a given value g_i insulates M_j from changes to the other generative factors \mathbf{G}_{-i} , and it is defined as:*

$$\text{PIDA}(G_i, M_j | g_i, \mathbf{g}_{-i}) := d(p_{\theta}(M_j | do(G_i \leftarrow g_i)), p_{\theta}(M_j | do(G_i \leftarrow g_i, \mathbf{G}_{-i} \leftarrow \mathbf{g}_{-i}))) \quad (3)$$

where d is a divergence.⁴ The average worst case over all possible choices of g_i and \mathbf{g}_{-i} is given by:

$$\text{EMPIDA}(G_i, M_j) := \mathbb{E}_{g_i} [\max_{\mathbf{g}_{-i}} \text{PIDA}(G_i, M_j | g_i, \mathbf{g}_{-i})] \quad (4)$$

Definition 3 (Disentanglement of representations) *We say that a representation \mathbf{M} is disentangled with respect to \mathbf{G} if and only if $\max_j \min_i \text{EMPIDA}(G_i, M_j)$ is exactly zero.*

In other words, \mathbf{M} is disentangled with respect to \mathbf{G} if, for every M_j there exists a G_i such that fixing the latter *insulates* M_j from changes to the other generative factors \mathbf{G}_{-i} . In section 4, we will build on both types of disentanglement to derive our notion of alignment between representations.

Another important notion is that of *context-style separation*, which can be viewed as a special case of disentanglement of representations von Kügelgen et al. [2021]. Let the generative factors \mathbf{G} be partitioned into two disentangled sectors $\mathbf{G}_{\mathcal{I}}$ and $\mathbf{G}_{-\mathcal{I}}$, representing task-relevant information (content) and task-irrelevant factors of variations (style), respectively. Then, \mathbf{M} satisfies content-style separation if the following holds:

Definition 4 (Content-style separation) *Let $(\mathbf{G}_{\mathcal{I}}, \mathbf{G}_{-\mathcal{I}})$ be two disentangled sectors. Then, \mathbf{M} separates content from style iff it can be partitioned into $(\mathbf{M}_{\mathcal{I}}, \mathbf{M}_{-\mathcal{I}})$ such that:*

$$\text{EMPIDA}(\mathbf{G}_{\mathcal{I}}, \mathbf{M}_{\mathcal{I}}) = 0 \quad (5)$$

This means that, if the content $\mathbf{G}_{\mathcal{I}}$ is fixed, the machine representation $\mathbf{M}_{\mathcal{I}}$ are isolated from changes to the style $\mathbf{G}_{-\mathcal{I}}$. This property is asymmetrical: it holds even if $\mathbf{M}_{-\mathcal{I}}$ is affected by interventions to $\mathbf{G}_{\mathcal{I}}$. Also, there is no requirement that the elements of $\mathbf{M}_{\mathcal{I}}$ are disentangled with respect to $\mathbf{G}_{\mathcal{I}}$.

⁴The original definition [Suter et al., 2019] fixes d to be the difference between means. Here, we slightly generalize PIDA to arbitrary divergences, as doing so can account for changes in higher-order moments too.

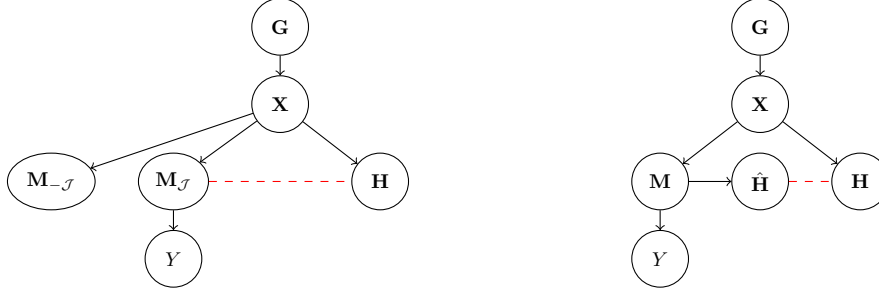


Figure 2: **Left:** generative process followed by concept-based models *CBMs*. A prediction is inferred based on a subset of “interpretable” concepts $\mathbf{M}_{\mathcal{J}} \subseteq \mathbf{M}$, so it is to $\mathbf{M}_{\mathcal{J}}$ that our notion of alignment (section 4, in **red**) applies. **Right:** generative process followed by *concept-based explainers* (CBEs). Here, the machine representation \mathbf{M} is *not* required to be interpretable. Rather, the explainer maps it to extracted concepts $\hat{\mathbf{H}}$ and then infers how these contribute to the prediction. Here it is $\hat{\mathbf{H}}$ that alignment applies to.

3 Human Interpretable Representation Learning

We are concerned with acquiring interpretable machine representations. Our key intuition is that a representation is only interpretable as long as it can be *understood by the human at the receiving end*. Based on this, we formally state our learning problem as follows:

Definition 5 *Human-interpretable representation learning (HRL) is the problem of learning a (possibly stochastic) mapping between inputs $\mathbf{x} \in \mathbb{R}^d$ and a set of machine representations $\mathbf{z} \in \mathbb{R}^k$ that enables a machine and a specific human stakeholder to communicate using those representations.*

This mapping can be modeled without loss of generality as a conditional distribution $p_{\theta}(\mathbf{Z} | \mathbf{X})$, whose parameters θ are estimated from data. While definition 5 encompasses both CBEs and CBMs, the meaning of \mathbf{Z} differs in the two cases, as we show next.

3.1 Machine Representations: The Ante-hoc Case

CBMs are neural predictors that follow the generative process shown in fig. 2 (left). During inference, a CBM observes an input \mathbf{x} , caused by generative factors \mathbf{G} , and extracts a representation \mathbf{M} by performing MAP inference [Koller and Friedman, 2009] on a distribution $p_{\theta}(\mathbf{M} | \mathbf{x})$ implemented as a neural network. This representation is partitioned into two subsets: $\mathbf{M}_{\mathcal{J}}$ are constrained to be interpretable, while $\mathbf{M}_{-\mathcal{J}}$ are not. As shown in fig. 2, only the interpretable subset is used for inferring a prediction \hat{y} , while $\mathbf{M}_{-\mathcal{J}}$ – if present – is used for other tasks, such as reconstruction [Marconato et al., 2022]. Specifically, the predicted concepts $\mathbf{M}_{\mathcal{J}}$ are fed to a simulatable top layer $p_{\theta}(Y | \mathbf{M})$ – most often a sparse linear layer – from which an explanation can be easily derived. Assuming $\mathbf{M}_{\mathcal{J}}$ is in fact interpretable, CBMs can provide local *explanations* summarizing what concepts are responsible for a particular prediction in an *ante hoc* fashion and essentially for free Bontempelli et al. [2021], Schwalbe [2022]. For instance, if $p_{\theta}(Y | \mathbf{M}_{\mathcal{J}})$ is a linear mapping with parameters w_{yj} , the explanation for predicting \hat{y} is given by Alvarez-Melis and Jaakkola [2018], Chen et al. [2019, 2020], Koh et al. [2020], Marconato et al. [2022], Zarlenga et al. [2022]:

$$\mathcal{E} = \{(w_{\hat{y}j}, m_j) : j \in \mathcal{J}\} \tag{6}$$

where each concept activation m_j is associated with a “level of responsibility” inferred from the top layer’s weights. Specific CBMs are outlined in section 6.

Summarizing, in the case of CBMs the concepts \mathbf{Z} used for communicating with users (cf. definition 5) are embodied by the interpretable machine representation $\mathbf{M}_{\mathcal{J}}$.

3.2 Machine Representations: The Post-hoc Case

For CBEs, the generative process is different, see fig. 2 (right). In this case, the internal representation \mathbf{M} of the model mapping from inputs \mathbf{X} to labels Y is *not required to be interpretable*. For instance, it

might represent the state of all neurons in a neural network or that of the neurons in the second-to-last layer. CBEs explain the reasoning process in a *post hoc* fashion by extracting the activations of high-level concepts $\hat{\mathbf{H}}$ from \mathbf{M} , and then inferring a concept-based explanation \mathcal{E} specifying the contribution of each \hat{H}_i to the model’s prediction, often in the same form as eq. (6).

Here, we are concerned with the interpretability of $\hat{\mathbf{H}}$. Some approaches extract them by (indirectly) relying on concept annotations. For instance, TCAV [Kim et al., 2018] takes a set of linear classifiers, one for each concept, pre-trained on a densely annotated dataset, and then adapts them to work with machine representation \mathbf{M} . Unsupervised approaches instead mine the concepts directly in the space of machine representations through a linear decomposition [Ghorbani et al., 2019, Zhang et al., 2021, Fel et al., 2023a,b]. Specific examples are discussed in section 6. In general, there is no guarantee that the symbolic and sub-symbolic representations $\hat{\mathbf{H}}$ and \mathbf{M} capture exactly the same information. This introduces a *faithfulness* issue, meaning that CBE explanations may not portray a reliable picture of the model’s inference process [Kim et al., 2018, Teso, 2019, Pfau et al., 2021, Fel et al., 2023b].

However, the issue we focus on is that the representation $\mathbf{Z} = \hat{\mathbf{H}}$ used by CBEs to communicate with users is in fact interpretable, regardless of whether it is also faithful.

3.3 From Symbolic Communication to Alignment

What makes symbolic communication possible? While a complete answer to this question is beyond the scope of this paper, we argue that communication becomes challenging unless the concepts \mathbf{Z} with which the machine and the human communicate are “*aligned*”, in the sense that concepts having the same *name* share the same (or similar enough) *semantics*. Other factors contributing to interpretability will be discussed in section 5.

In order to formalize this intuition, we focus on the generative process shown in fig. 3. In short, we assume observations \mathbf{x} – *e.g.*, images or text observed during training and test – are obtained by mapping generative factors $\mathbf{G} \sim p^*(\mathbf{G} | \mathbf{C})$ through a hidden ground-truth distribution $p^*(\mathbf{X} | \mathbf{G})$.

The observations \mathbf{x} are then received by *two observers*: a machine and a human. The machine maps them to its own learned representation \mathbf{M} , which may or may not be interpretable. The interpretable representations \mathbf{Z} – which correspond to $\mathbf{M}_{\mathcal{J}}$ for CBMs (cf. section 3.1) and to $\hat{\mathbf{H}}$ for CBEs (section 3.2) – is then derived from \mathbf{M} .

At the same time, the human observer maps the same observations to its own vocabulary of concepts \mathbf{H} . For instance, if \mathbf{x} is an image portraying a simple object on a black background, \mathbf{h} may encode the “color” or “shape” of that object, or any other properties deemed relevant by the human. The choice and semantics of these concepts depend on the background and expertise of the human observer and possibly on the downstream task the human may be concerned with (*e.g.*, medical diagnosis or loan approval), and as such may vary between subjects. It is to *these* concepts that the human associates names – like in fig. 4 – and it is these concepts that they would use for communicating the properties of \mathbf{x} to other people.

Notice that the human concepts \mathbf{H} may be arbitrarily different from the ground-truth factors \mathbf{G} : whereas the latter include all information necessary to determine the observations, and as such may be complex and uninterpretable [Gabbay et al., 2021], the former are those aspects of the observation that matter to the human observer. A concrete example is that of color blindness: an observer may be unable to discriminate between certain wavelengths of visible light, despite these being causes of the generated image \mathbf{X} . Another, more abstract, example are the generative factors that cause a particular apple to appear ripe, *e.g.*, those biological processes occurring during the apple tree’s reproductive cycle, which are beyond the understanding of most non-experts.⁵ In stark contrast, the concept of “redness” is not causally related to the apple’s appearance, and yet easily understood by most human observers, precisely because it is a feature that is evolutionarily and culturally useful to those observers. In this sense, *the concepts \mathbf{H} are understandable by definition*.

We argue that symbolic communication is feasible whenever the names associated (by the human) to elements of \mathbf{H} can be transferred to the elements of \mathbf{Z} in a way that preserves semantics. That is, *concepts with the same name should have the same meaning*. In order to ensure information expressed in terms of

⁵They are so opaque that a whole science had to be developed to identify and describe them.

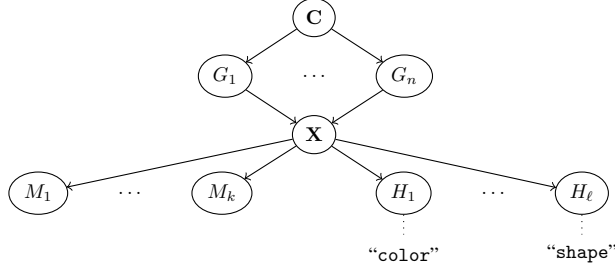


Figure 3: Graphical model of our data generation process. In words, n (correlated) generative factors exist in the world $\mathbf{G} = (G_1, \dots, G_n)$ that *cause* an observed input \mathbf{X} . The machine maps these to an internal representation $\mathbf{M} = (M_1, \dots, M_k)$, while the human observer maps them to its own internal concept vocabulary $\mathbf{H} = (H_1, \dots, H_\ell)$. Notice that the observer’s concepts \mathbf{H} may and often do differ from the ground-truth factors \mathbf{G} . The concepts \mathbf{H} are what the human can understand and attach names to, *e.g.*, the “color” and “shape” of an object appearing in \mathbf{X} . The association between names and human concepts is denoted by dotted lines. We postulate that communication is possible if the machine and the human representations are *aligned* according to definition 6.

\mathbf{Z} – say, an explanation stating that Z_1 is irrelevant for a certain prediction – is understood by the human observer, we need to make sure that \mathbf{Z} itself is somehow “aligned” with the human’s representation \mathbf{H} .

4 Alignment as Name Transfer

4.1 Alignment: The Disentangled Case

What does it mean for two representations to be aligned? We start by looking at the simplest (but non-trivial) case in which the ground-truth factors \mathbf{G} are *disentangled*, cf. definition 1. For ease of exposition, let us also temporarily assume that some of the generative factors are inherently interpretable, as in [Marconato et al., 2022]. Namely, we assume all factors in $\mathbf{G}_{\mathcal{I}} \subseteq \mathbf{G}$, where $\mathcal{I} \subseteq [n]$, can be understood by the human observer, while those in $\mathbf{G}_{-\mathcal{I}}$ cannot. The corresponding data generation process is illustrated in fig. 4. Under these assumptions, we aim to recover machine representations \mathbf{M} that are aligned to the interpretable factors $\mathbf{G}_{\mathcal{I}}$.

To this end, we generalize the notion of alignment introduced by Marconato et al. [2022].⁶ As anticipated, our definition revolves around the conditional distribution on \mathbf{M} given by \mathbf{G} , or equivalently the stochastic map $\alpha : \mathbf{g} \mapsto \mathbf{m}$ defined in eq. (2) and shown in **red** in fig. 4. The key intuition is that *two concept vocabularies \mathbf{G} and \mathbf{M} are aligned if and only if α preserves the semantics of the interpretable generative factors $\mathbf{G}_{\mathcal{I}}$.*

More specifically, alignment holds if α allows to *transfer the names* of the interpretable factors in a way that preserves semantics. If $p_\theta(\mathbf{M} | \mathbf{X})$ is learned in an unsupervised fashion, names are generally transferred by collecting or constructing inputs annotated with the corresponding human concepts, feeding them to the concept extractor, and looking for matches between the annotations and the elements of $\mathbf{M}_{\mathcal{J}}$.⁷ In a sense, this process is analogous to giving the human observer access to a set of “knobs”, each one controlling the value of one $G_i \in \mathbf{G}_{\mathcal{J}}$, and to a visualization of the machine representation $\mathbf{M}_{\mathcal{J}}$. Turning a knob is akin to *intervening* on the corresponding factor G_i . If, by turning a knob, the user is able to figure out what G_i corresponds to what M_j , then they will associate them the same name. Since we are assuming $\mathbf{G}_{\mathcal{I}}$ is disentangled, turning one knob does not affect the others, which simplifies the process.

The formal definition of alignment is as follows:

⁶Our definition extends that of [Marconato et al., 2022] to the general case in which the mapping α – which is defined as a marginal distribution in eq. (2) – is stochastic rather than deterministic. Doing so allows us to cater to more realistic applications and to draw an explicit connection with PIDA in proposition 1.

⁷If concept-level annotations are used, the names are automatically transferred along with them, but we still wish the user to be able to match the learned concepts with its own.

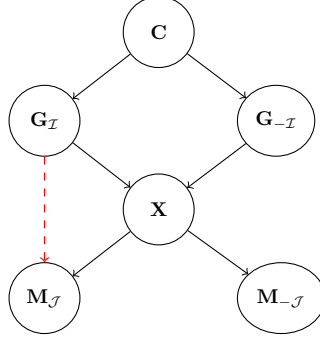


Figure 4: Simplified generative process with a single observer, adapted from [Marconato et al., 2022]. Here, \mathbf{C} are unobserved confounding variables influencing the generative factors \mathbf{G} , and \mathbf{M} is the latent representation learned by the machine. The **red** arrow represents the map α .

Definition 6 (Alignment) Given generative factors \mathbf{G} of which $\mathbf{G}_{\mathcal{I}}$ are interpretable, a machine representation \mathbf{M} is aligned iff the map α between \mathbf{G} and \mathbf{M} can be written as:

$$\mathbf{M}_{\mathcal{J}} = \alpha(\mathbf{G}, \mathbf{N})_{\mathcal{J}} = (\mu_j(G_{\pi(j)}, N_j) : j \in \mathcal{J}) \quad (7)$$

where $\mathbf{M}_{\mathcal{J}} \subseteq \mathbf{M}$ are the machine representations that ought to be interpretable, \mathbf{N} are independent noise variables, and π and μ satisfy the following properties:

D1. The index map $\pi : \mathcal{J} \mapsto \mathcal{I}$ is surjective and, for all $j \in \mathcal{J}$, it holds that, as long as $G_{\pi(j)}$ is kept fixed, M_j remains unchanged even when the other generative factors $\mathbf{G} \setminus \{G_{\pi(j)}\}$ are forcibly modified.

D2. Each element-wise transformation μ_j , for $j \in \mathcal{J}$, is monotonic in expectation over N_j :

$$\exists \bowtie \in \{>, <\} \text{ such that } \forall g'_{\pi(j)} > g_{\pi(j)}, \left(\mathbb{E}_{N_j}[\mu_j(g_{\pi(j)}, N_j)] - \mathbb{E}_{N_j}[\mu_j(g'_{\pi(j)}, N_j)] \right) \bowtie 0 \quad (8)$$

Let us motivate our two desiderata. In line with prior work on disentangled representations [Bengio et al., 2013, Higgins et al., 2018], **D1** requires that α should not “mix” multiple G_i ’s into a single M_j , regardless of whether the former belong to $\mathbf{G}_{\mathcal{I}}$ or not. For instance, if M_j blends together information about both color and shape, or about color and some uninterpretable factor, human observers would have trouble pinning down which one of their concepts it matches. If it does not, then turning the $G_{\pi(j)}$ knob only affects M_j , facilitating name transfer.⁸ We will show in section 4.2 that this is equivalent to disentanglement.

D2 is also related to name transfer. Specifically, it aims to ensure that, whenever the user turns a knob $G_{\pi(j)}$, they can easily understand *what* happens to M_j and thus figure out the two variables encode the same information. To build intuition, notice that both **D1** and **D2** hold for the *identity* function, as well as for those maps α that *reorder* or *rescale* the elements of $\mathbf{G}_{\mathcal{I}}$, which clearly preserve semantics and naturally support name transfer. Monotonicity captures all of these cases and also more expressive *non-linear* element-wise functions, while *conservatively* guaranteeing a human would be able to perform name transfer. Notice also that **D2** can be constrained further based on the application.

A couple of remarks are in order. Most importantly, notice that *our definition of alignment immediately applies also to the mapping between \mathbf{Z} and the human vocabulary \mathbf{H}* . In this case, α is the map between human concepts \mathbf{h} and machine representations \mathbf{z} , obtained by marginalizing over \mathbf{X} , \mathbf{G} , and \mathbf{C} (see fig. 3), and it is only aligned if it satisfies **D1** and **D2**. More generally, alignment can hold for *any* mapping between representations. We also observe that, since π maps \mathcal{J} exclusively into \mathcal{I} , alignment entails a form of *content-style separation* (definition 4), in that $\mathbf{M}_{\mathcal{J}}$ does not encode any information about $\mathbf{G}_{-\mathcal{I}}$. We will show in section 4.3 that representations that do not satisfy this condition can be affected by *concept leakage*, while aligned representations cannot. Finally, we note that \mathbf{M} can be aligned and still contain multiple transformations of the same $G_i \in \mathbf{G}_{\mathcal{I}}$. This does not compromise interpretability in that all “copies” can always be traced back to the same G_i .

⁸The converse is not true: as we will see in section 4.4, interpretable concepts with “compatible semantics” can in principle be blended together without compromising interpretability.

4.2 Disentanglement Does Not Entail Alignment

Next, we clarify the relationship between alignment and disentanglement of representations by showing that the latter is exactly equivalent to **D1**:

Proposition 1 *Assuming noise terms are independent, as per section 2, **D1** holds if and only if the representations are disentangled in $(\mathbf{G}_{\mathcal{I}}, \mathbf{M}_{\mathcal{J}})$ (cf. definition 3.)*

All proofs can be found in appendix A. The equivalence between disentanglement of representations and **D1** implies that *disentanglement is insufficient for interpretability*: even if \mathbf{M} is disentangled, *i.e.*, each M_j encodes information about at most one $G_i \in \mathbf{G}_{\mathcal{I}}$, nothing prevents the transformation from G_i to its associated M_j from being arbitrarily complex, complicating name transfer. In the most extreme case, $\alpha(\cdot)_j$ may not be *injective*, making it impossible to distinguish between different g_i ’s, or could be an arbitrary shuffling of the continuous line: this would clearly obfuscate any information present about G_i . This means that, during name transfer, a user would be unable to determine what value of M_j corresponds to what value of G_i or to anticipate how changes to the latter affect the former.

This is why **D2** in definition 6 requires the map between each $G_i \in \mathbf{G}_{\mathcal{I}}$ and its associated M_j to be “simple”. This extra desideratum makes alignment *strictly stronger* than disentanglement.

4.3 Alignment Entails No Concept Leakage

Concept leakage is a recently discovered phenomenon whereby the “interpretable” concepts $\mathbf{M}_{\mathcal{J}}$ unintentionally end up encoding information about extraneous concepts [Mahinpei et al., 2021]. Empirically, leaky concepts are predictive for inference tasks that – in principle – do not depend on them. Situations like the following occur in practice, even if full concept supervision is used [Marconato et al., 2022, Mahinpei et al., 2021, Margeloiu et al., 2021]:

Example 1 *Let \mathbf{X} be a dSprites image [Matthey et al., 2017] picturing a white sprite, determined by generative factors including “position”, “shape”, and “size”, on a black background. Now imagine training a concept extractor $p_{\theta}(\mathbf{M} | \mathbf{X})$ so that $\mathbf{M}_{\mathcal{J}}$ encodes shape and size – but not position – by using full concept-level annotations for shape and size. The concept extractor is then frozen. During inference, the goal is to classify sprites as either positive ($Y = 1$) or negative ($Y = 0$) depending on whether they are closer to the top-right corner or the bottom-left corner. When concept leakage occurs, the label – which clearly depends only on position – can be predicted with above random accuracy from $\mathbf{M}_{\mathcal{J}}$, meaning these concepts somehow encode information about position, which they are not supposed to.*

The only existing formal account of concept leakage was provided by Marconato et al. [2022], who view it in terms of (lack of) out-of-distribution (OOD) generalization. Other works instead focus on in-distribution behavior and argue that concept leakage is due to encoding discrete generative factors using a continuous representation [Lockhart et al., 2022, Havasi et al., 2022]. We go beyond these works by providing the first general formulation of concept leakage and showing that it is related to alignment. Specifically, we propose to view *concept leakage as a (lack of) content-style separation*, and show that this explains how concept leakage can arise both in- and out-of-distribution.

We start by formalizing the intuition that concept leakage is excess prediction accuracy – gained by leveraging leaky concepts – compared to a leak-free baseline [Marconato et al., 2022, Havasi et al., 2022]. The corresponding generative process is reported in fig. 5. We assume the generative factors \mathbf{G} are partitioned as $(\mathbf{G}_{\mathcal{I}}, \mathbf{G}_{-\mathcal{I}})$ such that only $\mathbf{G}_{-\mathcal{I}}$ are *informative* for predicting a label Y , mediated by the conditional distribution $p(Y | \mathbf{G}_{-\mathcal{I}})$. This implies that their mutual information is positive, that is, $I(\mathbf{G}_{-\mathcal{I}}, Y) > 0$.⁹ Now, fix a concept encoder $p_{\theta}(\mathbf{M}_{\mathcal{J}} | \mathbf{X})$ and let $q_{\lambda}(Y | \mathbf{M}_{\mathcal{J}})$ be a predictor learned on top of it (in orange in the figure). To quantify concept leakage, we look at how well the best possible such predictor can infer the label Y using $\mathbf{M}_{\mathcal{J}}$ after intervening on $\mathbf{G}_{-\mathcal{I}}$. Analogously to EMPIDA (definition 2), the intervention detaches $\mathbf{G}_{-\mathcal{I}}$ from \mathbf{C} , thus ensuring the label Y cannot be influenced by the irrelevant factors $\mathbf{G}_{\mathcal{I}}$. The resulting manipulated distribution on \mathbf{G} is:

$$p'(\mathbf{G}) = p(\mathbf{G} | do(\mathbf{G}_{-\mathcal{I}} \leftarrow \mathbf{g}_{-\mathcal{I}}))q(\mathbf{g}_{-\mathcal{I}}) := \mathbb{E}_{\mathbf{C}}[p(\mathbf{G}_{\mathcal{I}} | \mathbf{C})] \mathbb{1}\{\mathbf{G}_{-\mathcal{I}} = \mathbf{g}_{-\mathcal{I}}\} q(\mathbf{g}_{-\mathcal{I}}) \quad (9)$$

⁹In this section we are mostly concerned with the non-informativeness of $\mathbf{G}_{\mathcal{I}}$, hence we allow $\mathbf{G}_{-\mathcal{I}}$ to potentially contain also interpretable factors.

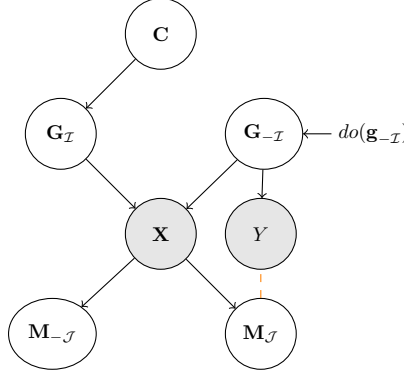


Figure 5: Generative process for Concept Leakage. A predictor observes examples (\mathbf{X}, Y) and infers Y from its interpretable representation $\mathbf{M}_{\mathcal{J}}$ using a learnable conditional distribution $q_{\lambda}(Y | \mathbf{m}_{\mathcal{J}})$, indicated in **orange**. Since the label Y depends solely on $\mathbf{G}_{-\mathcal{I}}$, we would expect that it *cannot* be predicted better than at random: intuitively, if this occurs it means that information from $\mathbf{G}_{-\mathcal{I}}$ has leaked into the interpretable concepts $\mathbf{M}_{\mathcal{J}}$. Any intervention $do(\mathbf{G}_{-\mathcal{I}} \leftarrow \mathbf{g}_{-\mathcal{I}})$ on the uninterpretable/unobserved concepts detaches these from \mathbf{C} , meaning that the label truly only depends on $\mathbf{G}_{-\mathcal{I}}$.

where $q(\mathbf{g}_{-\mathcal{I}})$ is a distribution over possible interventions. This can be *any* distribution, with the only requirement that under any intervention $do(\mathbf{G}_{-\mathcal{I}} \leftarrow \mathbf{g}_{-\mathcal{I}})$ the model observes different variations of Y .¹⁰

From the causal factorization in fig. 5, the joint probability of (\mathbf{X}, Y) resulting from the post-interventional distribution $p'(\mathbf{G})$ is given by:

$$p(\mathbf{X}, Y) = \mathbb{E}_{\mathbf{g} \sim p'(\mathbf{G} | do(\mathbf{G}_{-\mathcal{I}} \leftarrow \mathbf{g}_{-\mathcal{I}}))} [p(Y | \mathbf{g}_{-\mathcal{I}}) p(\mathbf{X} | \mathbf{g})] \quad (10)$$

Data of this kind appear, for example, in the dSprites experiment [Marconato et al., 2022] outlined in example 1. Here, during training the “position” of the sprite is fixed (*i.e.*, $\mathbf{G}_{pos} = \mathbf{G}_{-\mathcal{I}}$ are fixed to the center), while at test time the data contains different interventions over the position $\mathbf{G}_{pos} = \mathbf{G}_{-\mathcal{I}}$, and free variations of the other factors $\mathbf{G}_{\mathcal{I}}$ (*e.g.*, “shape” and “size”). Essentially, these interventions move the sprite around the top-right and bottom-left borders, where the factors \mathbf{G}_{pos} are extremely informative for the label Y .

In order to measure the degree of concept leakage in $p_{\theta}(\mathbf{M}_{\mathcal{J}} | \mathbf{X})$, we compare the prediction performance of the best possible predictor $q_{\lambda}(Y | \mathbf{M}_{\mathcal{J}})$ with that of the best possible predictor $r_{\gamma}(Y)$ that does not depend on $\mathbf{M}_{\mathcal{J}}$ at all. This is equivalent to comparing the behavior of two Bayes optimal predictors, one of which has access to the learned (possibly leaky) concepts whereas the other does not. In the following, we assume the distributions q_{λ} and r_{γ} to be sufficiently expressive, *i.e.*, they can encode any sufficiently well behaved stochastic function. This is the case, for instance, when they are implemented as deep neural networks. We are now ready to define concept leakage:

Definition 7 (Concept Leakage) Given a classifier $q_{\lambda}(y | \mathbf{z})$, an uninformed Bayes optimal predictor $r_{\gamma}(y)$, and data samples $(\mathbf{x}, y) \in \mathcal{D}$, concept leakage Λ is the difference:

$$\Lambda = \max_{\lambda} [\mathcal{L}_{CL}(\lambda)] - \max_{\gamma} [\mathcal{L}_r(\gamma)] \quad (11)$$

where:

$$\mathcal{L}_{CL} = \mathbb{E}_{(\mathbf{x}, y) \sim p(\mathbf{X}, Y)} \log q_{\lambda, \theta}(y | \mathbf{x}) \quad \mathcal{L}_r = \mathbb{E}_{(\mathbf{x}, y) \sim p(\mathbf{X}, Y)} \log r_{\gamma}(y) \quad (12)$$

are the average log-likelihood of the classifier $q_{\lambda, \theta}(Y | \mathbf{X}) := \mathbb{E}_{\mathbf{m}_{\mathcal{J}} \sim p_{\theta}(\mathbf{M}_{\mathcal{J}} | \mathbf{X})} p(Y | \mathbf{m}_{\mathcal{J}})$ and of the uninformed Bayes optimal classifier, respectively.

By definition 7, concept leakage occurs if and only if there exists a λ that allows to predict Y better than the best uninformed predictor. In the following analysis, we characterize concept leakage evaluated on the ground-truth distribution $p(\mathbf{X}, Y)$. We proceed to show that this quantity is bounded by two terms:

¹⁰If Y is constant, leakage is impossible, since $I(\mathbf{G}_{-\mathcal{I}}, Y) = 0$.

Proposition 2 Assuming the causal factorization in fig. 5, it holds that:

$$I(\mathbf{M}_{\mathcal{J}}, Y) \leq \Lambda \leq I(\mathbf{G}_{-\mathcal{I}}, Y) \quad (13)$$

where $I(\mathbf{A}, \mathbf{B})$ denotes the mutual information between \mathbf{A} and \mathbf{B} .

The bounds in eq. (13) are useful for understanding how concept leakage behaves. They show, for instance, that Λ cannot exceed the mutual information between $\mathbf{G}_{-\mathcal{I}}$ and Y . Second, applying the data-processing inequality [Cover, 1999] to the lower bound yields $I(\mathbf{M}_{\mathcal{J}}, Y) \geq I(\mathbf{M}_{\mathcal{J}}, \mathbf{G}_{-\mathcal{I}})$. The latter quantifies the information contained in $\mathbf{M}_{\mathcal{J}}$ about $\mathbf{G}_{-\mathcal{I}}$. In other words, concept leakage can only be zero if indeed the machine concepts $\mathbf{M}_{\mathcal{J}}$ contain no information about them, because $I(\mathbf{M}_{\mathcal{J}}, \mathbf{G}_{-\mathcal{I}}) \leq \Lambda = 0$. Next, we also show that if $\mathbf{M}_{\mathcal{J}}$ does not encode information about $\mathbf{G}_{-\mathcal{I}}$ – or equivalently, it satisfies content-style separation (definition 4) – then it has zero concept leakage.

Proposition 3 Suppose that $\mathbf{M}_{\mathcal{J}}$ does not encode any information of $\mathbf{G}_{-\mathcal{I}}$, consistently with content-style separation (definition 4), then Λ is zero.

This result leads to two consequences. Let us start by looking at the *out-of-distribution case* investigated in [Marconato et al., 2022]. Here, the concept extractor is trained only on some fixed variations of $\mathbf{G}_{-\mathcal{I}}$. However, when the support of $\mathbf{G}_{-\mathcal{I}}$ changes drastically, the model is not likely to ensure content-style separation outside of the support of the training distribution, even if **D1** holds in-distribution. This failure can be explained by the difficulty of disentanglement techniques to ensure disentanglement for out-of-distribution samples – in the context of combinatorial generalization – by Montero et al. [2020, 2022]. Consider for dSprites example. Here, during training, sprites are located in the dead center of the background, and when observing the sprites on the borders of the image, which is far away from the support of the training set, the concept encoder fails to ensure their representations are disentangled. This failure of disentanglement techniques to ensure disentanglement for out-of-distribution inputs was also observed – in the context of combinatorial generalization – by Montero et al. [2020, 2022]. Our results show that if content-style separation does not hold, concept leakage may be non-zero, meaning that techniques like open-set recognition [Sun et al., 2020] must be adopted to detect OOD inputs and process them separately.

Next, we look at concept leakage for *in-distribution* scenarios. Following Havasi et al. [2022], consider a model leveraging two concepts – presence of “tail” and “fur” – and the task of distinguish between images of cats and dogs using these (clearly non-discriminative) concepts. According to [Havasi et al., 2022], concept leakage can occur when binary concepts like these are modelled using continuous variables, meaning the concept extractor can unintentionally encode “spurious” discriminative information. In light of our analysis, we argue that concept leakage is instead due to lack of content-style separation, and thus of alignment. To see this, suppose there exists a concept $G_k \in \mathbf{G}_{-\mathcal{I}}$ useful for distinguishing cats from dogs and that it is disentangled as in definition 1 from the concepts of fur G_{fur} and of tail G_{tail} . Then, by content-style separation, any representation $\mathbf{M}_{\mathcal{J}}$ that is aligned to G_{fur} and G_{tail} does not encode any information about G_k , leading to zero concept leakage.

In both cases, concept leakage arises as a failure in content-style separation between relevant and irrelevant generative factors, and as such it can be used as a proxy for measuring the latter. Moreover, since alignment implies content-style separation, aligned representations cannot suffer from concept leakage.¹¹

An extension of this result includes the case where $G_k \in \mathbf{G}_{\mathcal{I}}$, *i.e.*, the ground-truth factor G_k is relevant for in-distribution predictions Y and representations $\mathbf{M}_{\mathcal{J}}$ encode it somewhere. In this case, concept leakage is evaluated among the elements of $\mathbf{M}_{\mathcal{J}}$ that should not encode G_k . That is, if a subset of $\mathbf{M}_{\mathcal{J}}$ encodes only the concepts G_{fur} and G_{tail} it must not be discriminative for Y . Without loss of generality,¹² we suppose that only a single $M_{j'}$ is aligned to G_k , that is $\pi(j') = k$, whereas other $\mathbf{M}_{\mathcal{J}} \setminus M_{j'}$ are aligned to other concepts, among which G_{fur} and G_{tail} . Then, the following holds:

Corollary 1 Consider a representation $\mathbf{M}_{\mathcal{J}}$ that is aligned to a set of disentangled concepts $\mathbf{G}_{\mathcal{I}}$, among which only G_k is discriminative for the label Y . Then, all $M_j \in \mathbf{M}_{\mathcal{J}}$ that are not associated by α to G_k , *i.e.*, $\pi(j) \neq k$, do not suffer from concept leakage.

¹¹Note that the converse is not true: while alignment entails content-style separation, the latter can hold independently from alignment.

¹²The general case includes all representations $\mathbf{M}_{\pi^{-1}(k)}$, where π^{-1} is the pre-image of the map π .

Ultimately, an aligned representation prevents concept leakage among the encoded concepts. If some of the representations $\mathbf{M}_{\mathcal{J}}$ are aligned only to the concepts G_{fur} and G_{tail} , they cannot be used to discriminate between *cats* and *dogs*.

4.4 Alignment: The Block-wise Case

So far, we assumed the generative factors $\mathbf{G}_{\mathcal{I}}$ – or, equivalently, the human concepts \mathbf{H} – are disentangled. We now extend alignment to more complex cases in which the human concepts *can* be mixed together without compromising interpretability. This covers situations in which, for instance, the machine captures a single categorical generative factor using multiple variables via one-hot encoding, or uses polar coordinates to represent the 2D position of an object.

To formalize this setting, we assume $\mathbf{G}_{\mathcal{I}}$ and $\mathbf{M}_{\mathcal{J}}$ are partitioned into non-overlapping “blocks” of variables $\mathbf{G}_{\mathcal{I}'} \subseteq \mathbf{G}_{\mathcal{I}}$ and $\mathbf{M}_{\mathcal{J}'} \subseteq \mathbf{M}_{\mathcal{J}}$, respectively. The idea is that each block $\mathbf{M}_{\mathcal{J}'}$ captures information about only a single block $\mathbf{G}_{\mathcal{I}'}$, and that while mixing across blocks is not allowed, mixing the variables within each block *is*. From the human’s perspective, this means that name transfer is now done block by block. With this in mind, we define *block alignment* as follows:

Definition 8 (Block-wise Alignment) *A machine representation \mathbf{M} is block-wise aligned to $\mathbf{G}_{\mathcal{I}}$ if and only if there exists a subset $\mathbf{M}_{\mathcal{J}} \subseteq \mathbf{M}$, a partition $\mathcal{P}_{\mathbf{M}}$ of \mathcal{J} , and a mapping $\alpha : (\mathbf{g}, \mathbf{N}) \mapsto \mathbf{m}$ such that:*

$$\mathbf{M}_{\mathcal{J}'} = \alpha(\mathbf{G}, \mathbf{N})_{\mathcal{J}'} := \mu_{\mathcal{J}'}(\mathbf{G}_{\Pi(\mathcal{J}')}, \mathbf{N}_{\mathcal{J}'}) \quad \forall \mathcal{J}' \in \mathcal{P}_{\mathbf{M}} \quad (14)$$

where the maps Π and μ satisfy the following properties.

D1 *There exists a partition $\mathcal{P}_{\mathbf{G}}$ of \mathcal{I} ¹³ such that $\Pi : \mathcal{P}_{\mathbf{M}} \rightarrow \mathcal{P}_{\mathbf{G}}$. We call this condition block-wise disentanglement*

D2 *Each map $\mu_{\mathcal{J}'}$ is simulatable and invertible¹⁴ on the first statistical moment, that is, there exists a unique pre-image α^{-1} defined as:*

$$\mathbf{G}_{\Pi(\mathcal{J}')} = \alpha^{-1}(\mathbb{E}[\mathbf{M}_{\mathcal{J}}])_{\mathcal{J}'} := \left(\mathbb{E}_{\mathbf{N}_{\mathcal{J}'}}[\mu_{\mathcal{J}'}(\cdot, \mathbf{N}_{\mathcal{J}'})] \right)^{-1}(\mathbf{G}_{\Pi(\mathcal{J}')}) \quad (15)$$

By **D1**, changes to any block of human concepts only impact a single block of machine concepts, and by **D2** the change can be anticipated by the human observer, that is the human interacting with the machine grasps what is the general mechanism behind the transformation from \mathbf{G} (or \mathbf{H}) and \mathbf{M} (and vice versa). Both properties support name transfer.

A priori, it is not clear to say what transformations are simulatable [Lipton, 2018], as this property depends crucially on the human’s cognitive limitations and knowledge. However, simulatability can be assessed via user studies in practice. We remark that **D2** implicitly constraints the variables within each block to be “semantically compatible” because this property impacts simulatable. In the context of image recognition, for instance, placing concepts such as “nose shape” and “sky color” in the same block is likely to make name transfer substantially more complicated, as changes to “nose shape” might end affecting the representation of “sky color”. Semantic compatibility is fundamentally a psychological issue. An example of semantic compatibility is that of rototranslation of the coordinates followed by element-wise rescaling¹⁵. A counter example would be a map α given by a conformal map for the 2D position of an object in a scene. Albeit invertible, it may not be simple at all to simulate.

Notice that with this definition we include two possible scenarios: (i) the case where some of the ground-truth concepts belonging to the same block are transformed in a single block, and (ii) the case where semantically compatible, but disentangled, concepts $\mathbf{G}_{\mathcal{I}}$ are mixed together in $\mathbf{M}_{\mathcal{J}}$, which is often neglected in current disentanglement literature. The latter includes and extends the special case of alignment for disentangled \mathbf{G} .

The limitation of definition 8 reflects the fact that taking into account the possible user’s grasp of the representation is not straightforward to define and poses a challenge to provide a uniquely accepted definition that considers the human factor.

¹³In principle, we can extend this notion to a family of subsets $\mathcal{P}_{\mathbf{G}}$ of \mathcal{I} . As an example, for *xyz* positions, one can consider blocks $\{xy, yz, xz\}$ that are mapped to respectively block aligned representations.

¹⁴For continuous variables, we require it to be a diffeomorphism.

¹⁵This condition is identical to “weak identifiability” in representation learning Hyvarinen and Morioka [2017], Khemakhem et al. [2020a].

4.5 Alignment: The General Case

In the most general case the generative factors \mathbf{G} are causally related to each other according to an arbitrary ground-truth SCM $\mathcal{C}_{\mathbf{G}}$. This entails that $\mathbf{G}_{\mathcal{T}}$ is no longer (block) disentangled. Hence, during name transfer turning a “knob” (*i.e.*, a variable G_i) affects those knobs that are causally dependent on it.

Naturally, the semantics of the user’s comprises the causal relations between them. To see this, let G_1 be the temperature and G_2 the color of a metal object: the user knows that temperature affects color, and would not assign the same name to a representation of temperature that does not have a similar effect on the representation of color. In order ensure preservation of these semantics, we say that a machine representation \mathbf{M} is *aligned* to \mathbf{G} if, whenever the human intervenes on one G_i , affecting those generative factors $\mathbf{G}_{\mathcal{T}'}$ that depend on it, an analogous change occurs in the machine representation.

We now show that *block-alignment* is sufficient to satisfy this desideratum. Even in this more general case, the distribution over the representation can be obtained by marginalizing over the input variables:

$$p(\mathbf{M}) := \mathbb{E}_{\mathbf{x} \sim p(\mathbf{x})} p_{\theta}(\mathbf{M} | \mathbf{x}) \equiv \mathbb{E}_{\mathbf{g} \sim p(\mathbf{G})} p_{\theta}(\mathbf{M} | \mathbf{g}) \quad (16)$$

Notice that the definition of block alignment does not make any assumption about absence or presence of causal relations between blocks of generative factors, meaning that we it is still well-defined in this more general setting.¹⁶ Specifically, a map α can be block aligned if the variables G within each block are disentangled with each other, although there may exist causal relations across blocks.

Now, imagine having a stochastic map α between \mathbf{G} and \mathbf{M} that does satisfy block alignment, and also that there exist causal relations between the blocks $\mathbf{G}_{\mathcal{T}'}$. Whenever the user turns a “knob” corresponding to a ground-truth block, this yields an interventional distribution $p(\mathbf{G} | do(\mathbf{G}_{\mathcal{T}'} \leftarrow \mathbf{g}_{\mathcal{T}'}))$. Through α , this determines a new interventional distribution on the machine representations, namely:

$$p(\mathbf{M} | do(\mathbf{G}_{\mathcal{T}'} \leftarrow \mathbf{g}_{\mathcal{T}'})) = \mathbb{E}_{\mathbf{g} \sim p(\mathbf{G} | do(\mathbf{G}_{\mathcal{T}'} \leftarrow \mathbf{g}_{\mathcal{T}'}))} p_{\theta}(\mathbf{M} | \mathbf{g}) \quad (17)$$

This implies a representation \mathbf{M} where the (interventional) distribution is obtained by mapping the state $\mathbf{g}_{\mathcal{T}'}$ through α . The same operation can be performed to obtain the state of all other machine representations aligned with the blocks that are causally related to $\mathbf{G}_{\mathcal{T}'}$ and affected by the intervention.

Note that this distribution *automatically takes causal relations between generative factors into account and treats them as causal relations between machine representations*. To see this, consider the following example:

Example 2 Consider two generative factors G_1 and G_2 causally connected via a structural assignment $G_2 \leftarrow f(G_1, N_2)$, as in fig. 6. As before, G_1 could be the temperature and G_2 the color of a metal solid. Correspondingly, the aligned representation \mathbf{M} encodes the temperature in two distinct variables, M_1 and M_3 , respectively to the temperature, say, measured in Celsius and Fahrenheit degrees. M_2 encodes the color variable.

The consequence of block-wise alignment is sketched in the fig. 6 in three distinct cases: (left) intervening on the temperature G_1 affects both the aligned variables (M_1, M_3) and the color G_2 . Correspondingly this has an effect also on M_2 that changes according to G_2 . (center) An intervention on G_2 influences only M_2 through α and it does not affect M_1 and M_3 . (right) The effect of an intervention on whole variables \mathbf{G} is localized such that interventions on the temperature factor G_1 will affect M_1 and M_3 , whereby the interventions on G_2 only affect M_2 , isolating it from the intervention on G_1 .

Next, we formalize our observation that, thanks to *block alignment*, interventions on \mathbf{G} are automatically mirrored on \mathbf{M} :

Proposition 4 Given a block-wise aligned representation \mathbf{M} to \mathbf{G} , it holds that for each distinct block $\mathbf{M}_{\mathcal{K}}$ of representations \mathbf{M} , an intervention on $\mathbf{G}_{\Pi(\mathcal{K})}$ isolates $\mathbf{M}_{\mathcal{K}}$ from interventions of other ground-truth blocks $\mathbf{G}_{-\Pi(\mathcal{K})}$. Moreover, distinct interventions on $\mathbf{G}_{\Pi(\mathcal{K})}$ corresponds on average to different interventions on $\mathbf{M}_{\mathcal{K}}$.

Importantly, this means that the effect of an intervention on the whole \mathbf{G} isolates each block in \mathbf{M} from the others, *i.e.*, there is no explicit causal relation appearing in the learned representation. This matches the intuition that an intervention on a specific generative factor affects the corresponding block and removes the dependencies on other blocks of the representation.

¹⁶This generalizes block alignment beyond disentangled factors [Suter et al., 2019].

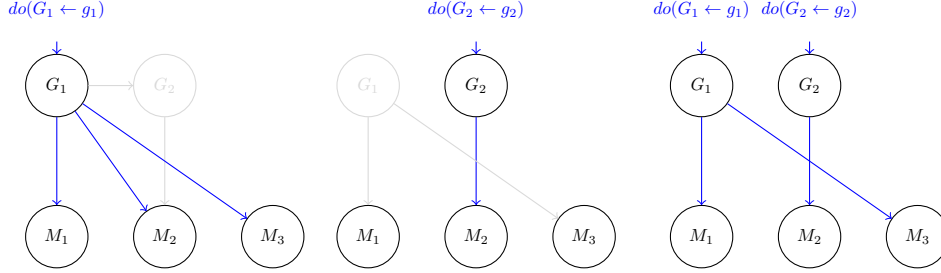


Figure 6: **Block-aligned representation** when $\mathcal{C}_{\mathbf{G}}$ has causal connections. (left) An intervention on G_1 affects all representation (displayed in blue), since (M_1, M_3) are block-aligned to G_1 and M_2 is aligned to G_2 . (center) Conversely, an intervention on G_2 only affects M_2 , leaving the remaining representations untouched. (right) Intervening on all \mathbf{G} has the effect of isolating the corresponding aligned representations from other interventions. In this case, intervening on G_2 removes the causal connection with G_1 , so that M_2 does not depend on the intervention of G_1 . Refer to example 2 for further details.

Summarizing, block alignment entails interventions to the ground-truth concepts are mapped properly. At the same time, alignment between blocks ensures the transformation α is simulatable, meaning that users can understand changes happening to all of the variables involved. This is sufficient to guarantee name transfer can be completed successfully in the general case, assuming not too many factors are changed at a time.

4.6 Alignment and Causal Abstractions

One important observation is that the form of name transfer we have considered is *asymmetrical*, in the sense that the user intervenes on its own representation \mathbf{H} only, to then check how this impacts \mathbf{M} . The other direction is not considered: it is not necessary to consider how intervening on \mathbf{M} impacts \mathbf{M} . This leads to the setup depicted in fig. 7 (right) in which, given $\mathcal{C}_{\mathbf{H}}$, the effects of interventions on H_i are propagated to \mathbf{M} via a map $\beta : \mathbf{H} \mapsto \mathbf{M}$, which may or may not be block-aligned.

We now consider a scenario in which the SCM of the representation $\mathcal{C}_{\mathbf{M}}$ is also provided¹⁷ and the effects of interventions on \mathbf{M} can be propagated leveraging its structural assignments.

Ideally, we would expect that, as long as \mathbf{M} is block-aligned to \mathbf{H} , we can always find analogous post-interventional effects when intervening on H_i and on its aligned variable M_j . This underlies a consistency condition between the two “worlds” that are described with $\mathcal{C}_{\mathbf{H}}$ and $\mathcal{C}_{\mathbf{M}}$, respectively, by requiring that they both lead to similar conclusions when intervened in an equivalent manner. Clearly, this does not depend solely on the nature of the map β but also on the structure of the machine SCM $\mathcal{C}_{\mathbf{M}}$.

The presence of a consistency property between $\mathcal{C}_{\mathbf{H}}$ and $\mathcal{C}_{\mathbf{M}}$ is what defines a *causal abstraction* [Beckers and Halpern, 2019, Beckers et al., 2020, Rubenstein et al., 2017], cf. [Zennaro, 2022] for an overview. Causal abstractions have been proposed to define (approximate) equivalence between causal graphs and have recently been employed in the context of explainable AI [Geiger et al., 2023b,a]. The existence of a causal abstraction ensures two systems are *interventionally equivariant*: interventions on one system can always be mapped (modulo approximations) to equivalent interventions in the other and lead to the same interventional distribution.

All causal abstractions check the consistency between two maps under the same intervention $do(\mathbf{H}_{\mathcal{I}})$: one is defined by the post-interventional distribution of $\mathcal{C}_{\mathbf{H}}$ that is mapped on \mathbf{M} via β , the other one consists of first matching on \mathbf{M} the correspondent action $do(\mathbf{M}_{\mathcal{I}})$ and propagate it via $\mathcal{C}_{\mathbf{M}}$. Intuitively, this means that, under β , interventions on \mathbf{H} lead to the same conclusion as interventions on \mathbf{M} . We formalize this idea from constructive causal abstractions¹⁸ [Geiger et al., 2023b] by adapting it to the case where \mathbf{H} and \mathbf{M} are connected by block-alignment:

¹⁷In practice, $\mathcal{C}_{\mathbf{M}}$ can be uncovered from data via causal discovery [Pearl, 2009].

¹⁸Existing works on causal abstractions [Beckers and Halpern, 2019, Geiger et al., 2023b] do not impose the map between values or interventions are simulatable, meaning that even if $\mathcal{C}_{\mathbf{M}}$ is a causal abstraction of $\mathcal{C}_{\mathbf{H}}$, it may be impossible for users to understand the mapping between the two.

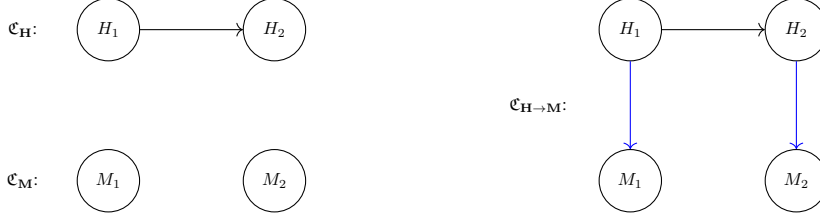


Figure 7: **Absence of Aligned Causal Abstraction.** (left) The user’s \mathcal{C}_H incorporates a causal connection between H_1 to H_2 , while the machine one \mathcal{C}_M presents no causal connections. (right) The total SCM $\mathcal{C}_{H \rightarrow M}$ of user’s and machine’s concepts resulting from an **aligned** map $\beta : \mathbf{H} \rightarrow \mathbf{M}$ (in blue). Refer to example 3 for further discussion.

Definition 9 (β -Aligned Causal Abstraction) The \mathcal{C}_M is a causal abstraction of \mathcal{C}_H under block-alignment β if, for all possible interventions $do(\mathbf{H}_{\mathcal{I}} \leftarrow \mathbf{h}_{\mathcal{I}})$ with $\mathbf{H}_{\mathcal{I}} \subseteq \mathbf{H}$, the following diagram commutes:

$$\begin{array}{ccc}
do(\mathbf{H}_{\mathcal{I}} \leftarrow \mathbf{h}_{\mathcal{I}}) & \xrightarrow{\mathcal{C}_H} & p(\mathbf{H} \mid do(\mathbf{H}_{\mathcal{I}} \leftarrow \mathbf{h}_{\mathcal{I}})) \\
\downarrow \beta & & \downarrow \beta_* \\
do(\mathbf{M}_{\mathcal{J}} \leftarrow \mathbf{m}_{\mathcal{J}}) & \xrightarrow{\mathcal{C}_M} & p(\mathbf{M} \mid do(\mathbf{M}_{\mathcal{J}} \leftarrow \mathbf{m}_{\mathcal{J}}))
\end{array} \tag{18}$$

where β_* denotes the push-forward operation applied to the probability $p(\mathbf{H} \mid do(\mathbf{H}_{\mathcal{I}} \leftarrow \mathbf{h}_{\mathcal{I}}))$, and $\mathcal{J} = \Pi^{-1}(\mathcal{I})$ is the pre-image of \mathcal{I} under Π .

In other words, aligned causal abstractions extend block alignment by enforcing a *symmetrical* consistency condition over interventions when both SCMs \mathcal{C}_H and \mathcal{C}_M are known: interventions on \mathbf{M} have analogues on \mathbf{H} and vice-versa. This becomes relevant in situations where the user cannot parse the effect of an intervention on H_i on the input \mathbf{X} , *i.e.*, they do not have access to $p(\mathbf{X} \mid do(H_i \leftarrow h_i))$, and they are left to validate the effects of their actions through β . In this case, leveraging on the SCM \mathcal{C}_M , the user can check how the mirrored intervention on M_j spreads in the machine representations, and compare it with the corresponding representations given by β when the intervention is propagated on the user’s factors \mathbf{H}_{-i} .

Therefore, while a map β being aligned is a necessary condition, it is not sufficient to guarantee a successful *name transfer* if \mathcal{C}_M is highly dissimilar from \mathcal{C}_H . We show this situation explicitly where, despite having alignment between the user and the machine, the consistency condition in eq. (18) does not hold.

Example 3 We consider two SCMs, one over user variables \mathcal{C}_H and one over the machine ones \mathcal{C}_M . As shown in fig. 7 (left), the two SCMs have a different structure and for ease of reference we refer to H_1 and M_1 as the *temperature* variable and to H_2 and M_2 as the *color* variable. Despite the different structure, we suppose M_1 and M_2 are aligned to H_1 and H_2 , respectively, via an aligned map β . We indicate the overall causal graph as $\mathcal{C}_{H \rightarrow M}$, see fig. 7 (right).

We can now check that \mathcal{C}_M is not an aligned abstraction of \mathcal{C}_H under β . In fact, intervening on H_1 leads to different results on \mathcal{C}_M and $\mathcal{C}_{H \rightarrow M}$. For the former, changing the temperature amounts to modify only the corresponding variable M_1 and does not affect M_2 , as evident in fig. 7 (left). Conversely, a change in the temperature under alignment corresponds also to a change in color for the variable M_2 , as depicted in fig. 7 (right). The two interventional effects, hence, do not coincide and \mathcal{C}_M is not an aligned causal abstraction of \mathbf{H} .

5 Discussion and Limitations

Our work provides a crisp requirement that machine representations should satisfy to ensure interpretability, namely *alignment* with the human’s concept vocabulary. Next, we address important issues arising from this requirement.

5.1 Is Perfect Alignment Sufficient and Necessary?

It is natural to ask whether perfect alignment is a *sufficient* and *necessary* condition for interpretability of machine concepts. Recall that alignment is born out of two desiderata. The first one is that of *subjectivity*: a concept is understandable *to* a particular human observer, with different observers having different expertise and knowledge. This is captured by the human’s vocabulary \mathbf{H} in our definition. The second one is that of guaranteeing that *machine and human concepts sharing the same name also share the same semantics*, translated into the desideratum that whenever a human concept changes the human can anticipate how this will change the machine representation. For instance, if the human and the machine see the same picture of a dog, the *human* can easily figure out what concept encodes the notion of “dog” and how it would change if they were to delete the dog from the picture.¹⁹

Is alignment sufficient? Simply ensuring that two agents share aligned representations does not automatically entail that symbolic communication will be successful. For instance, a human observer may misinterpret a machine explanation built out of aligned concepts simply due to inattention, confusion, or information overload. These are all important elements in the equation of interpretability, and we do not intend to dismiss them. The way in which information is *presented* is about as important as the *contents* of the information being conveyed. The problem of designing interfaces that ensure the presentation is engaging and easy to understand is however beyond the scope of this paper. This does not impact our core message, that is, that *lack* of alignment can severely hamper communication and that therefore approaches for learning and evaluating conceptual representations should be designed with this requirement in mind.

Is alignment necessary? We also point out that perfect alignment is not strictly *necessary*, for two reasons. First, it is enough that alignment holds only *approximately*. Slight differences in semantics between machine and human concepts are unlikely to have major effects on communication. This is compatible with the empirical observation that people can often successfully communicate even without fully agreeing on the semantics of the words they exchange [Marti et al., 2023]. In practice, the degree of misalignment, and its impact of the communication, can be defined and measured, at which point the maximum allowed misalignment becomes an application-specific variable. Second, it may not be necessary that alignment holds *everywhere*. If two agents exchange only a subset of possible messages (e.g., explanations), concepts not appearing in those messages need not be aligned. For instance, ensuring a CBM classifying apples as ripe or not to be interpretable only requires the concepts appearing in its explanations to be aligned, and possibly only those values that actually occur in the explanations (e.g., `color = red` but not `color = blue`). This can be understood as a more lax form of alignment applying only to a certain subset of (values of) the generative factors $\mathbf{g}_{\mathcal{I}}$, e.g., those related to apples. It is straightforward to relax definition 6 in this sense by restricting it to a subset of the support of $p^*(\mathbf{G}_{\mathcal{I}})$ from which the inputs \mathbf{X} are generated, as these constrain the messages that the two agents can exchange.

5.2 Measuring Alignment

While there exist several metrics for measuring interpretability of concepts (discussed in section 6.4), here we are concerned with techniques for assessing *alignment*.

Considering the relation between alignment and disentanglement (**D1**), one option is to leverage one of the many measures of disentanglement proposed in the literature [Zaidi et al., 2020]. The main issues is that most of them provide little information about how simple the map α (**D2**) is and as such they cannot be reused as-is. However, for the disentangled case (cf. section 4.1), Marconato et al. [2022] noted that one can measure alignment using the linear DCI [Eastwood and Williams, 2018]. Essentially, this metric checks whether there exists a *linear regressor* that, given $\mathbf{m}_{\mathcal{J}}$, can predict $\mathbf{g}_{\mathcal{I}}$ with high accuracy, such that each M_j is predictive for at most one G_i . In practice, doing so involves collecting a set of annotated pairs $\{(\mathbf{m}_{\mathcal{J}}, \mathbf{g}_{\mathcal{I}})\}$, where the m_j ’s and g_i ’s are rescaled in $[0, 1]$, and fitting a linear regressor on top of them using L_1 regularization. DCI then considers the (absolute values of the) regressor coefficients $B \in \mathbb{R}^{|\mathcal{J}| \times |\mathcal{I}|}$ and evaluates average dispersion of B_j : for each machine representation M_j . In short, if each M_j predicts only a single G_i , and with high accuracy, then linear DCI is maximal. The key insight is that the existence of such a linear map implies both disentanglement (**D1**) and monotonicity (**D2**), and therefore also alignment. The main downside is that the converse does not hold, that is, linear DCI cannot account for non-linear monotonic relationships.

¹⁹This last point takes into account, at least partially, the limited cognitive processing abilities of human agents.

The alternative we advocate is that of *decoupling* the measurement of **D1** and **D2**, and to leverage causal notions for the former. **D1** can for instance be measured using the *interventional robustness score* (IRS) [Suter et al., 2019], an empirical version of EMPIDA (definition 2) that – essentially – measures the average effect of interventions on $\mathbf{G}_{\mathcal{I}}$ on the machine representation. Alternatives include, for instance, DCI-ES Eastwood et al. [2022], which can better capture the degree by which factors are mixed and the mutual information gap (MIG) [Chen et al., 2018]. These metrics allow to establish an empirical map π between indices of the human and machine representations, using which it is possible to evaluate **D2** separately. One option is that of evaluating Spearman’s rank correlation between the distances:

$$|g_i - g'_i|^2 \quad \text{and} \quad \|\mathbb{E}[\mathbf{M}_{\mathcal{J}} \mid do(G_i \leftarrow g_i)] - \mathbb{E}[\mathbf{M}_{\mathcal{J}} \mid do(G_i \leftarrow g'_i)]\|_2^2 \quad (19)$$

for interventions g_i and g'_i , leaving \mathbf{G}_{-i} fixed, for each $i \in \mathcal{I}$ and multiple traversals (g_i, g'_i) .

Unfortunately, none of the existing metrics are suited for non-disentangled generative factors $\mathbf{G}_{\mathcal{I}}$ or human representations \mathbf{H} , which are central for alignment in the block-wise (section 4.4) and general (section 4.5) cases. We leave an in-depth study of more generally applicable metrics to future work.

5.3 Consequences for Concept-based Explainers

Recall that CBEs explain the predictions of black-box models by extracting interpretable concepts $\hat{\mathbf{H}}$ from the model’s internal representation \mathbf{M} and then evaluating their contribution to the prediction (cf. section 3.1). In this case, the requirement is that $\hat{\mathbf{H}}$ is aligned to the human’s concept vocabulary \mathbf{H} – irrespective of how the former is extracted. Notice that *alignment* is orthogonal to *faithfulness*, in the sense that an aligned representation can be unfaithful to the model, and a faithful representation misaligned with the human. In other words, *alignment is a property of the map from \mathbf{H} to $\hat{\mathbf{H}}$, while faithfulness is a property of the map between \mathbf{M} and $\hat{\mathbf{H}}$.*

If the mapping from \mathbf{M} to $\hat{\mathbf{H}}$ is *invertible*, then it is always possible map back and forth – in a lossless manner – from the machine representations \mathbf{M} to the surrogate $\hat{\mathbf{H}}$. This is a solid basis for faithfulness: whatever information is conveyed by an explanation built on $\hat{\mathbf{H}}$ can always be cast in terms of the machine representation itself,²⁰ and that whatever relation the latter has with the prediction can be mapped in terms of human concepts.

In the general case, however, it is non-trivial to find a suitable invertible function. Suppose the user provides the machine with annotated examples $(\mathbf{x}_i, \mathbf{h}_i)$ and that these are used – as is common with supervised CBEs, see section 6.2 – to learn the mapping from \mathbf{M} to $\hat{\mathbf{H}}$. Ensuring that this is invertible requires potentially an enormous amount of examples. To see this, consider a simple case in which the human concepts \mathbf{H} are binary and disentangled and that \mathbf{M} and \mathbf{H} are related by a (possibly complex) invertible mapping that is not an alignment. Even in this ideal case, it might take up to 2^ℓ examples – where ℓ is the dimension of \mathbf{H} – to align the two representations, as this involves finding the correct permutation from \mathbf{M} to \mathbf{H} . Alignment can help in this regard. In fact, if \mathbf{M} is aligned to \mathbf{H} , the number of required examples scales as $\mathcal{O}(\ell)$, because a single intervention to each user concept H_i is sufficient to find the corresponding aligned element M_j .

In summary, not only do unaligned (black-box) models imply CBEs require more supervision on the user concepts to acquire a invertible transformation ensuring faithfulness, but also it is likely that the representation \mathbf{M} mixes together the interpretable factors $\mathbf{G}_{\mathcal{I}}$ with the non-interpretable ones $\mathbf{G}_{-\mathcal{I}}$, making it more difficult to extract a concepts $\hat{\mathbf{H}}$ aligned to \mathbf{H} .

5.4 Consequences for Concept-based Models

As discussed in section 6.1, most CBMs acquire concepts using a variety of heuristics that do not guarantee alignment. To the best of our knowledge, GlanceNets [Marconato et al., 2022] are the only CBM that *explicitly* optimizes for alignment, and as such avoids concept leakage. They do so by combining a variational auto-encoder mapping from the input \mathbf{X} to a machine representation $\mathbf{M} = (\mathbf{M}_{\mathcal{J}}, \mathbf{M}_{-\mathcal{J}})$ where only the first partition is used for prediction. These are computed using a simple linear layer, as is customary. The variational-auto encoder is trained with some amount of concept-level annotations. This encourages both disentanglement [Locatello et al., 2019] and monotonicity – and hence alignment

²⁰The resulting explanation may no longer be simple or understandable, but it still contains all the information of the original message.

– for *in-distribution* data. In turn, this also prevents concept leakage. In order to avoid leakage for *out-of-distribution* data, GlanceNets also implement an *open-set recognition* step [Sun et al., 2020]. This is responsible for detecting inputs encoding concepts that have never been observed during training. Whenever these are detected, GlanceNets refuse to output a prediction for them, thus avoiding leakage altogether.

From our perspective, GlanceNets have two major downsides. First, they are designed to seek alignment with respect to the generative factors underlying the observations. As we argued, however, interpretability requires alignment with respect to the human’s concept vocabulary. Second, GlanceNets require a moderate but non-trivial number of annotations. How to acquire them from the human observer remains an open problem, discussed in section 5.5.

Summarizing, GlanceNets could be repurposed for solving alignment in the disentangled case discussed in section 4.1 by combining them with a suitable annotation elicitation procedure. They are however insufficient to solve disentanglement when the ground-truth concepts are not disentangled, and new solutions will be necessary to tackle these more complex and realistic settings.

5.5 Collecting Human Annotations

Both metrics and learning strategies for alignment require some amount of annotations for the human factors \mathbf{H} . This is a core requirement related to the subjective nature of interpretability. One option is that of distributing the annotation effort among crowd-workers, which however is impractical for prediction tasks that require specific types of expertise, like medical diagnosis. An alternative is that of gathering together annotations from different online resources of large language models [Oikarinen et al., 2022]. Doing so, however, can lead to a lack of completeness (a necessary concept might be missing) and ambiguity (concepts annotations might mix together different views or meanings). This kind of supervision cannot guarantee alignment to a specific human observer.

Reducing the annotation effort for personalized supervision is challenging. Under the assumption that of leveraging generic concept annotations obtained using the above methods to pre-train the concept extractor, and then fine-tune the resulting model using a small amount of personalized annotations. This strategy can save annotation effort as long as the generic annotations contain most of the information necessary to retrieve the observer’s concepts. An alternative is to leverage concept-level interactive learning [Lage and Doshi-Velez, 2020, Chauhan et al., 2023], to request annotations only for those concepts that are less *aligned*. Naturally, one might also consider combining these two strategies, that is, interleaving fine-tuning with interactive learning, for additional gains. How to estimate alignment (or some lower bound thereof) in absence of full concept annotations is however an open research question and left to future work.

6 Related Work

While concepts lie at the heart of AI [Muggleton and De Raedt, 1994], the problem of acquiring *interpretable* concepts has historically been neglected in representation learning [Bengio et al., 2013]. Recently concepts have regained popularity in many areas of research, including explainable AI [Guidotti et al., 2018], neuro-symbolic AI [De Raedt et al., 2020], and causality [Pearl, 2009, Schölkopf et al., 2021], yet most concept acquisition strategies developed in these areas are only concerned with task accuracy, rather than interpretability. Next, we briefly overview strategies for acquiring interpretable representations and highlight their shortcomings for properly solving human-interpretable representation learning.

6.1 Unsupervised Approaches

A first group of strategies learn concepts directly from unlabeled data. Well-known theoretical results in deep latent variable models cast doubts on the possibility of acquiring representations satisfying *any* property of interest – including *disentanglement* and *interpretability* – in a fully unsupervised manner in absence of a strong architectural bias [Locatello et al., 2019, Khemakhem et al., 2020b]. This stems from the fact that, as long as the concept extraction layers are “flexible enough” (*i.e.*, have no strong architectural bias), predictors relying interpretable and uninterpretable concepts can achieve the very same accuracy (or likelihood) on both the training and test sets. As a consequence, *unsupervised strategies that*

only maximize for accuracy cannot guarantee interpretability unless they are guided by an appropriate bias. The main challenge is determining what this bias should be.

Several, mutually incompatible alternatives have been proposed. Unsupervised CBEs discover concepts in the space of neuron activations of a target model. One common bias is that concepts can be retrieved by performing a *linear decomposition* of the machine’s representation [Fel et al., 2023b]. Specific techniques include k-means [Ghorbani et al., 2019], principal component analysis [Graziani et al., 2023], and non-negative matrix factorization [Zhang et al., 2021, Fel et al., 2023a]. Concept responsibility is then established via feature attribution methods.

Two common biases used in CBMs are *sparsity* and *orthonormality*. Self-Explainable Neural Networks [Alvarez-Melis and Jaakkola, 2018] encourage the former by pairing an autoencoder architecture for extracting concepts from the input together with a (simulatable [Lipton, 2018]) task-specific prediction head, and then combining a cross-entropy loss with a penalty term encouraging concepts to have sparse activation patterns. Concept Whitening [Chen et al., 2020] implements a special bottleneck layer that ensures learned concepts are *orthogonal*, so as to minimize mutual information between them and facilitate acquiring concepts with disjoint semantics, as well as *normalized* within comparable activation ranges. The relationship between sparsity, orthonormality, and interpretability is however unclear.

Based on the observation that humans tend to reason in terms of concrete past cases [Kim et al., 2016], other CBMs constrain concepts to capture salient training examples or parts thereof, *i.e.*, *prototypes*. Methods in this group include Prototype Classification Networks [Li et al., 2018], Part-Prototype Networks [Chen et al., 2019], and many others [Rymarzyk et al., 2021, Nauta et al., 2021, Singh and Yow, 2021, Davoudi and Komeili, 2021]. At a high level, they all memorize one or more prototypes (*i.e.*, points in latent space) that match training examples of their associated class only. Predictions are based on the presence or absence of a match with the learned prototypes. The interpretability of this setup has however been called into question [Hoffmann et al., 2021, Xu-Darme et al., 2023]. The key issue is the matching step, which is carried out in latent space. The latter is generally underconstrained, meaning that prototypes can end up matching parts of training examples that carry no useful semantics (*e.g.*, arbitrary combinations of foreground and background) as long as doing so yields high training accuracy.

None of these approaches takes the human’s own concept vocabulary \mathbf{H} into account.

6.2 Supervised Strategies

A second family of approaches leverages concept *annotations* (or some form of weak supervision). Among supervised CBEs, Net2vec [Fong and Vedaldi, 2018] defines linear combinations of convolutional filters, and fits a linear model to decide whether their denoised saliency maps encode a given concept or not, yielding a binary segmentation mask. TCAV [Kim et al., 2018] defines concepts as directions – or concept-activation vectors (CAVs) – in latent space. These are obtained by adapting the parameters of per-concept linear classifiers trained on a separate densely annotated data set to the machine’s embedding space. Concept attributions are proportional to the degree by which changing their activations affects the prediction. Zhou et al. [2018] also relies on CAVs, but computes explanation by solving an optimization problem. A second group of supervised CBEs makes use of non-linear maps instead [Kazhdan et al., 2020, Gu and Tresp, 2019, Esser et al., 2020]. For instance, CME [Kazhdan et al., 2020] uses all activations of the model to learn categorical concepts via semi-supervised multi-task learning, while INN [Esser et al., 2020] fits a normalizing flow from the machine representation to the concepts so as to guarantee their relationship is bijective. Similarly, supervised CBMs like Concept-Bottleneck Models [Koh et al., 2020], Concept Whitening [Chen et al., 2020], and GlanceNets [Marconato et al., 2022], among others [Yuksekgonul et al., 2022, Sawada and Nakamura, 2022, Zarlenga et al., 2022] define a loss training penalty, for instance a cross-entropy loss, encouraging the extracted concepts to predict the annotations.

This solution seems straightforward: there is no more direct way than concept supervision to guide the model toward acquiring representations with the intended semantics. It also circumvents the negative theoretical results outlined in section 6.1.

However, models that accurately match the supervision do not necessarily satisfy content-style separation or allow to have disentangled representations, which – as discussed in section 4.3 – would lead to a non-negligible amount of *concept leakage* [Margeloiu et al., 2021, Mahinpei et al., 2021]. In contrast, alignment explicitly takes both properties into account. Another major issue is the supervision itself, which is frequently obtained from general sources rather than from the human observer them-

selves, meaning the learned concepts may not be aligned to the concept vocabulary of the latter. Two notable exceptions are the interactive concept learning approaches of Lage and Doshi-Velez [2020] and of Erculiani et al. [2023], which are however unconcerned with concept leakage.

To the best of our knowledge, GlanceNets [Marconato et al., 2022] are the only CBM that explicitly optimizes for alignment, and as such avoid leakage, yet they do so with respect to generative factors rather than human concepts. As discussed in section 5.4, however, GlanceNets can in principle be adapted to solve human-interpretable representation learning by combining them with a suitable annotation acquisition strategy. We plan to pursue this possibility in future work.

6.3 Disentanglement

Another relevant area of research is that on learning disentangled representations. Here, the goal is to uncover “meaningful”, independent factors of variation underlying the data [Higgins et al., 2016, 2018, Locatello et al., 2019], with the hope that these are also interpretable [Bengio et al., 2013]. Most current learning strategies rely on extensions of variational auto-encoders (VAEs) [Kingma and Welling, 2014, Higgins et al., 2016, Kim and Mnih, 2018, Chen et al., 2018, Esmaeili et al., 2019, Rhodes and Lee, 2021]. As anticipated in section 6.1, unless suitable architectural bias is provided, unsupervised learning cannot guarantee the learned representations are disentangled. Motivated by this, follow-up works seek disentanglement via either concept supervision [Locatello et al., 2020a], weak supervision [Shu et al., 2020, Locatello et al., 2020b], and other techniques [Lachapelle et al., 2022, Horan et al., 2021, Stammer et al., 2022]. Disentanglement however is unconcerned with the human’s concept vocabulary, and furthermore it is weaker than alignment, in that it does not readily support name transfer.

Independent component analysis (ICA) also seeks to acquire independent factors of variation [Comon, 1994, Hyvärinen et al., 2001, Naik and Kumar, 2011]. These assume the generative factors are independent from each other and determine an observation via an injective or invertible map. The objective of ICA is to recover the generative factors from the observations. While the linear case is well understood [Comon, 1994], the non-linear case is arguably more difficult. It was shown that *identifying* the ground truth factor is impossible in the unsupervised setting [Hyvärinen and Pajunen, 1999]. This is analogous to the results mentioned in section 6.1 and in fact a formal link between deep latent variable models and identifiability has recently been established. [Khemakhem et al., 2020b]. On the positive side, it is possible to show that providing auxiliary supervision on the factors guarantees identification up to permutation and negation, a property known as *strong identifiability*. *Weak identifiability* [Buchholz et al., 2022] relaxes it whereby the generative factors are recovered up to a transformation of the form $A\mathbf{g} + \mathbf{b}$, where $\text{rank}(A) \geq \min(\dim \mathbf{G}, \dim \mathbf{M})$ and \mathbf{M} is the machine representation and \mathbf{b} is an offset. Hyvärinen and Morioka [2017] also contemplate *identifiability up to element-wise non-linearities*, that is, given by the class of transformations $A\sigma[\mathbf{g}] + \mathbf{b}$, where σ can be a non-linear. If σ is restricted to be monotonic and A is an element-wise transformation, according to condition **D1** in definition 6, then this form of identifiability matches that of alignment in the disentangled case. However, this formulation refers to identification of the generative factors, while alignment is defined specifically in terms of human concepts. Moreover, we do not assume the map from human to machine concepts to be injective, nor to be exact.

6.4 Metrics of Concept Quality

Several metrics have been proposed for assessing the quality of extracted concepts and of explanations built on them. Standard measures include accuracy and surrogates thereof [Kim et al., 2018], Jaccard similarity [Fong and Vedaldi, 2018], sparsity, stability and ability to reconstruct the model’s internal representation [Fel et al., 2023b], and the degree by which concepts constitute a sufficient statistics for the prediction [Yeh et al., 2020]. We refer to [Schwalbe, 2022] for an overview. These metrics, however, either entirely neglect the role of the human observer – in that concept annotations are either not used or not obtained from the observer themselves – or fail to account for disentanglement and concept leakage. Alignment fills these gaps. Recently, two new metrics have been proposed to measure the concept impurity across individual learnt concepts and among sets of representations [Zarlenga et al., 2023], but the relation with alignment has not been uncovered yet.

There also exist a number of metrics for measuring disentanglement, such as β -VAE score [Higgins et al., 2016], Factor-VAE score [Kim and Mnih, 2018], mutual information gap [Chen et al., 2018], DCI [Eastwood and Williams, 2018], and IRS [Suter et al., 2019]. DCI provides also information about the

informativeness of its estimate, and – following [Marconato et al., 2022], it can be repurposed to measure a form of alignment where the μ transformations are linear definition 6. Suter et al. [2019] propose EMPIDA to analyze disentanglement from a causal perspective, upon which we base the construction of alignment. As mentioned in section 5.2, these metrics can be used to evaluate **D1** in the definition of alignment, and therefore alignment itself when paired with a metric for measuring the complexity of α (**D2**). Their properties are extensively discussed in Zaidi et al. [2020].

6.5 Neuro-Symbolic Architectures

The decomposition between low-level perception – that is, mapping inputs to concepts, also known as *neural predicates* in this setting – and high-level inference outlined in section 3.1 applies also to many neuro-symbolic (NeSy) models. Examples include DeepProbLog [Manhaeve et al., 2018], Logic Tensor Networks [Donadello et al., 2017], and related architectures [Diligenti et al., 2017, Fischer et al., 2019, Giunchiglia and Lukasiewicz, 2020, Yang et al., 2020, Huang et al., 2021, Marra and Kuželka, 2021, Ahmed et al., 2022, Misino et al., 2022, Winters et al., 2022, van Krieken et al., 2022, Ciravegna et al., 2023]. The biggest differences between CBMs and NeSy architectures is how they implement the top layer: the former rely on simulatable layers, while the latter on reasoning layers that take prior symbolic knowledge into account and are not necessarily simulatable.

Recent works [Marconato et al., 2023a,b] showed that learning a NeSy model consistent with prior knowledge using only label supervision is insufficient to guarantee the neural predicates capture the intended semantics. For instance, it is not uncommon that NeSy architectures attain high prediction accuracy by acquiring neural predicates that encode information about distinct and unrelated concepts. Interpretability of the *neural predicates* however also requires alignment, meaning that our results apply to these NeSy architectures as well.

7 Conclusion

Motivated by the growing importance of interpretable representations for both *post-hoc* and *ante-hoc* explainability, we have introduced and studied the problem of *human-interpretable representation learning*. Our key intuition is that concepts are interpretable only as long as they support symbolic communication with an interested human observer. Based on this, we developed a formal notion of alignment between distributions, rooted in causality, that ensures concepts can support symbolic communication and that applies to both *post-hoc* concept-based explainers and concept-based models. In addition, we clarified the relationship between alignment and the well-known notions of disentanglement, illustrating why the latter is not enough for interpretability, and uncovered a previously unknown link between alignment and concept leakage. Finally, looking at alignment in the most general case, we also unearthed its link to causal abstractions, which further cements the link between interpretability and causality and that we plan to expand on in future work. With this paper, our aim is that of bridging the gap between the human and the algorithmic sides of interpretability, with the hope of providing a solid, mathematical ground on which new research on human-interpretable representation learning can build.

Acknowledgements

We acknowledge the support of the MUR PNRR project FAIR - Future AI Research (PE00000013) funded by the NextGenerationEU. The research of ST and AP was partially supported by TAILOR, a project funded by EU Horizon 2020 research and innovation programme under GA No 952215.

A Proofs

A.1 Proof of Proposition 1

The proof requires to average over the confounds \mathbf{C} , encompassing the general case where different G 's may be correlated. To this end, we define the distributions $p(\mathbf{g}) = \mathbb{E}_{\mathbf{C}}[p(\mathbf{G})]$ and $p(\mathbf{G} \mid do(G_i \leftarrow g_i)) = \mathbb{1}\{G_i = g_i\} \mathbb{E}_{\mathbf{C}}[p(\mathbf{G}_{-i} \mid \mathbf{C})]$.

The proof is split into two parts: (i) proving that **D1** implies disentanglement, and (ii) the other way around.

(i) Assume that **D1** holds. Then, the conditional distribution of \mathbf{M} can be written as:

$$p_\theta(\mathbf{m}_{\mathcal{J}} \mid \mathbf{g}) = \prod_{j \in \mathcal{J}} p_\theta(m_j \mid g_{\pi(j)}) \quad (20)$$

We proceed to show that eq. (20) is disentangled in $(\mathbf{G}_{\mathcal{I}}, \mathbf{M}_{\mathcal{J}})$. For each $j \in \mathcal{J}$, it holds that the minimum value of $\text{EMPIDA}(G_i, M_j)$ is obtained when $i = \pi(j)$. That is because:

$$\begin{aligned} p_\theta(M_j \mid do(G_{\pi(j)} \leftarrow g_{\pi(j)})) &= \mathbb{E}_{\mathbf{g}_{-\pi(j)}} [p_\theta(M_j \mid g_{\pi(j)})] \\ p_\theta(M_j \mid do(G_{\pi(j)} \leftarrow g_{\pi(j)}, \mathbf{G}_{-\pi(j)} \leftarrow \mathbf{g}_{-\pi(j)})) &= p_\theta(M_j \mid g_{\pi(j)}) \end{aligned} \quad (21)$$

Note that the first distribution is independent of $\mathbf{g}_{-\pi(j)}$, so it is equivalent to the latter. Hence, $\text{EMPIDA}(G_{\pi(j)}, M_j)$ vanishes $\forall j \in \mathcal{J}$, yielding the claim.

(ii) Let now $\mathbf{M}_{\mathcal{J}}$ be disentangled with respect to $\mathbf{G}_{\mathcal{I}}$, that is:

$$\max_{j \in \mathcal{J}} \min_{i \in \mathcal{I}} \text{EMPIDA}(G_i, M_j) = 0 \quad (22)$$

which is verified *iff* it holds that $\min_{i \in \mathcal{I}} \text{EMPIDA}(G_i, M_j) = 0$ for all j . We now proceed by contradiction to show that vanishing EMPIDA is only consistent with **D1**. Suppose there exist at least one $j \in \mathcal{J}$ such that:

$$\alpha(\mathbf{m}_{\mathcal{J}})_j = \mu_j(\mathbf{g}_{-\mathcal{I}}, N_j) \quad (23)$$

where $\mathcal{K} \subseteq \mathcal{I}$ containing at least two elements. Therefore, the probability distribution for M_j can be written in general as $p(m_j \mid \mathbf{g}_{\mathcal{K}})$. Plugging this condition in the evaluation of EMPIDA we obtain for every $k \in \mathcal{K}$:

$$\begin{aligned} p(M_j \mid do(G_k \leftarrow g_k)) &= \mathbb{E}_{\mathbf{g}_{\mathcal{K} \setminus \{k\}}} [p_\theta(m_j \mid g_k, \mathbf{g}_{\mathcal{K} \setminus \{k\}})] \\ p(M_j \mid do(G_k \leftarrow g_k, \mathbf{G}_{-k} \leftarrow \mathbf{g}'_{-k})) &= p_\theta(m_j \mid g_k, \mathbf{g}'_{\mathcal{K} \setminus \{k\}}) \end{aligned} \quad (24)$$

Then, the two distributions coincide, and EMPIDA is zero, *iff* there exists a $k \in \mathcal{K}$ such that all possible interventions $\mathbf{G}_{\mathcal{K} \setminus \{k\}} \leftarrow \mathbf{g}'_{\mathcal{K} \setminus \{k\}}$ do not deviate from the expected distribution, formally:

$$\forall \mathbf{g}'_{\mathcal{K} \setminus \{k\}} \quad p(m_j \mid g_k, \mathbf{g}'_{\mathcal{K} \setminus \{k\}}) = \mathbb{E}_{\mathbf{g}_{\mathcal{K} \setminus \{k\}}} p_\theta(m_j \mid \mathbf{g}_{\mathcal{K}}) \quad (25)$$

which holds *iff* $p_\theta(m_j \mid \mathbf{g}_k, \mathbf{g}_{\mathcal{K} \setminus \{k\}}) = p_\theta(m_j \mid g_k)$, which is a contradiction. This proves the claim.

A.2 Proof of Proposition 2

In the following, we adopt the shorthand $\mathbf{m} = \mathbf{m}_{\mathcal{J}}$, and reintroduce the dependency on $\mathbf{m}_{-\mathcal{J}}$ at the end. First, we show that the maximum of the second term in Λ in eq. (12) coincides with the Shannon entropy of Y :

$$\begin{aligned} \mathcal{L}_r(\gamma) &= \mathbb{E}_{p(\mathbf{x}, y)} [\log r_\gamma(y)] \\ &= \int p(\mathbf{x}, y) \log r_\gamma(y) \, d\mathbf{x} dy \\ &= \int p(y) \log \frac{r_\gamma(y)p(y)}{p(y)} \, dy \\ &= -H(Y) - \text{KL}(p(Y) \parallel r_\gamma(Y)) \end{aligned} \quad (26)$$

where $p(Y)$ denotes the marginal distribution of Y , $H(Y)$ is the Shannon entropy given by $p(Y)$, and KL is the Kullback-Leibler divergence. Since the KL is always non-negative, the previous equation yields the upper bound:

$$\max_{\gamma} [\mathcal{L}_r(\gamma)] = -H(Y) \quad (27)$$

We proceed similarly to obtain a lower-bound:

$$\begin{aligned}
\mathcal{L}_{CL}(\lambda) &= \int p(\mathbf{x}, y) \log \left(\int q_\lambda(y | \mathbf{m}) p_\theta(\mathbf{m} | \mathbf{x}) d\mathbf{m} \right) dx dy \\
&\geq \int p(\mathbf{x}) p_\theta(\mathbf{m} | \mathbf{x}) p(y | \mathbf{x}) \log q_\lambda(y | \mathbf{m}) dx d\mathbf{m} dy \\
&= \int p_\theta(\mathbf{m}, y) \log q_\lambda(y | \mathbf{m}) d\mathbf{m} dy \\
&= \int p_\theta(\mathbf{m}, y) \log \frac{q_\lambda(y | \mathbf{m}) p_\theta(\mathbf{m}) p(y) p_\theta(\mathbf{m}, y)}{p_\theta(\mathbf{m}) p(y) p_\theta(\mathbf{m}, y)} d\mathbf{m} dy \\
&= \int p_\theta(\mathbf{m}, y) \log p(y) d\mathbf{m} dy + \int p_\theta(\mathbf{m}, y) \left[\log \frac{q_{\lambda, \theta}(\mathbf{m}, y)}{p_\theta(\mathbf{m}, y)} + \log \frac{p_\theta(\mathbf{m}, y)}{p_\theta(\mathbf{m}) p(y)} \right] d\mathbf{m} dy \\
&= -H(Y) - \text{KL}(p_\theta(\mathbf{M}, Y) || q_{\lambda, \theta}(\mathbf{M}, Y)) + I(\mathbf{M}, Y)
\end{aligned} \tag{28}$$

where $p_\theta(\mathbf{m}, y) = \int p(\mathbf{x}) p_\theta(\mathbf{m} | \mathbf{x}) p(y | \mathbf{x}) dx$, $p_\theta(\mathbf{m})$ is the posterior of the encoding distribution, $q_{\lambda, \theta}(\mathbf{m}, y) := q_\lambda(y | \mathbf{m}) p_\theta(\mathbf{m})$ denotes the joint probability, and $I(\mathbf{M}, Y)$ is the mutual information for the random variables \mathbf{M} and Y , distributed according to $p_\theta(\mathbf{M}, y)$. Maximizing the lower-bound implies learning a predictor $q_\lambda(y | \mathbf{m})$ that minimizes the KL term. By the previous equation this happens iff $q_\lambda(y, \mathbf{m})$ matches $p_\theta(\mathbf{m}, y)$. The lower-bound for the first term of Λ hence becomes:

$$\max_\lambda [\mathcal{L}_{CL}(\lambda)] \geq -H(Y) + I(\mathbf{M}, Y) \tag{29}$$

Adding this term to the second one shows retrieves the definition of concept leakage and shows that it is lower-bounded by:

$$\Lambda \geq I(\mathbf{M}_{\mathcal{J}}, Y) \tag{30}$$

We now proceed deriving the upper-bound for the first term:

$$\begin{aligned}
\mathcal{L}_{CL}(\lambda) &= \int p(\mathbf{x}, y) \log \left(\int q_\lambda(y | \mathbf{m}) p_\theta(\mathbf{m} | \mathbf{x}) d\mathbf{m} \right) dx dy \\
&= \int p(\mathbf{g}_{\mathcal{I}}) q(\mathbf{g}_{-\mathcal{I}}) \left[\int p(\mathbf{x} | \mathbf{g}) p(y | \mathbf{g}_{-\mathcal{I}}) \log \left(\int q_\lambda(y | \mathbf{m}) p_\theta(\mathbf{m} | \mathbf{x}) d\mathbf{m} \right) dx dy \right] d\mathbf{g}_{\mathcal{I}} d\mathbf{g}_{-\mathcal{I}} \\
&\leq \int q(\mathbf{g}_{-\mathcal{I}}) \left[\int p(y | \mathbf{g}_{-\mathcal{I}}) \log q_{\lambda, \theta}(y | \mathbf{g}_{-\mathcal{I}}) dy \right] d\mathbf{g}_{-\mathcal{I}} \\
&= \int q(\mathbf{g}_{-\mathcal{I}}) \left[\int p(y | \mathbf{g}_{-\mathcal{I}}) \log \frac{q_{\lambda, \theta}(y | \mathbf{g}_{-\mathcal{I}}) p(y) p(y | \mathbf{g}_{-\mathcal{I}}) q(\mathbf{g}_{-\mathcal{I}})}{p(y) p(y | \mathbf{g}_{-\mathcal{I}}) q(\mathbf{g}_{-\mathcal{I}})} dy \right] d\mathbf{g}_{-\mathcal{I}} \\
&= \int p(y) \log p(y) dy + \int q(\mathbf{g}_{-\mathcal{I}}) p(y | \mathbf{g}_{-\mathcal{I}}) \log \left[\frac{q_{\lambda, \theta}(y | \mathbf{g}_{-\mathcal{I}})}{p(y | \mathbf{g}_{-\mathcal{I}})} + \frac{p(y, \mathbf{g}_{-\mathcal{I}})}{p(y) q(\mathbf{g}_{-\mathcal{I}})} \right] dy d\mathbf{g}_{-\mathcal{I}} \\
&= -H(Y) - \mathbb{E}_{\mathbf{g}_{-\mathcal{I}} \sim q(\mathbf{g}_{-\mathcal{I}})} [\text{KL}(p(Y | \mathbf{G}_{-\mathcal{I}}) || q_{\lambda, \theta}(Y | \mathbf{G}_{-\mathcal{I}}))] + I(\mathbf{G}_{-\mathcal{I}}, Y)
\end{aligned} \tag{31}$$

where in the second line we decomposed $p(\mathbf{x}, y)$ with the data generation process, and in the third line we made use of Jensen inequality when bringing $\int p(\mathbf{x} | \mathbf{g}_{\mathcal{I}}) p(\mathbf{g}_{\mathcal{I}}) dx d\mathbf{g}_{\mathcal{I}}$ in the logarithm, and we denoted with $q_{\lambda, \theta}(y | \mathbf{g}_{-\mathcal{I}})$ the conditional distribution obtained by marginalizing over all expectations in the logarithm. Overall, the only part depending on λ appears in the KL term and $I(\mathbf{G}_{-\mathcal{I}}, Y)$ is the mutual information for the probability distribution $p(y | \mathbf{g}_{-\mathcal{I}}) q(\mathbf{g}_{-\mathcal{I}})$. Notice that the maximum of the upper-bound for $\mathcal{L}_{CL}(\lambda)$ corresponds to a vanishing KL term and hence the upper-bound for Λ results in:

$$\Lambda \leq I(\mathbf{G}_{-\mathcal{I}}, Y) \tag{32}$$

Finally, we arrive at the claim:

$$I(\mathbf{M}_{\mathcal{J}}, Y) \leq \Lambda \leq I(\mathbf{G}_{-\mathcal{I}}, Y) \tag{33}$$

which concludes the proof.

A.3 Proof of Proposition 3

D1 in definition 6 entails that the conditional probability of $\mathbf{M}_{\mathcal{J}}$ can be written in general as:

$$p_\theta(\mathbf{m}_{\mathcal{J}} | \mathbf{g}) = p_\theta(\mathbf{m}_{\mathcal{J}} | \mathbf{g}_{\mathcal{I}}) \tag{34}$$

The same holds for **D1** in definition 8. We make use of this fact for deriving a different upper-bound for Λ . We focus only on the first term of eq. (11); the analysis of the second one does not change.

$$\begin{aligned}
\mathcal{L}_{CL}(\lambda) &= \int p(\mathbf{x}, y) \log \left(\int q_\lambda(y | \mathbf{m}_{\mathcal{J}}) p_\theta(\mathbf{m}_{\mathcal{J}} | \mathbf{x}) d\mathbf{m}_{\mathcal{J}} \right) dx dy \\
&= \int p'(\mathbf{g}) \left[\int p(\mathbf{x} | \mathbf{g}) p(y | \mathbf{g}_{-\mathcal{I}}) \log \left(\int q_\lambda(y | \mathbf{m}_{\mathcal{J}}) p_\theta(\mathbf{m}_{\mathcal{J}} | \mathbf{x}) d\mathbf{m}_{\mathcal{J}} \right) dx dy \right] d\mathbf{g} \\
&\leq \int q(\mathbf{g}_{-\mathcal{I}}) \left[\int p(y | \mathbf{g}_{-\mathcal{I}}) \log \left(\int q_\lambda(y | \mathbf{m}_{\mathcal{J}}) p_\theta(\mathbf{m}_{\mathcal{J}} | \mathbf{g}_{\mathcal{I}}) p(\mathbf{g}_{\mathcal{I}}) d\mathbf{m}_{\mathcal{J}} d\mathbf{g}_{\mathcal{I}} \right) dy \right] d\mathbf{g}_{-\mathcal{I}} \\
&= \int p(y) \log p_{\lambda, \theta}(y) dy \\
&= \int p(y) \log \frac{p_{\lambda, \theta}(y) p(y)}{p(y)} dy \\
&= -H(Y) - \text{KL}(p(Y) || p_{\lambda, \theta}(Y))
\end{aligned} \tag{35}$$

In the second line we decomposed the data generation process, in the third line we made use of Jensen's inequality to introduce in the logarithm the term $\int p(\mathbf{g}_{\mathcal{I}}) d\mathbf{g}_{\mathcal{I}} \int p(\mathbf{x} | \mathbf{g}) dx$. The marginalization of $p_\theta(\mathbf{m}_{\mathcal{J}} | \mathbf{x})$ with $p(\mathbf{x} | \mathbf{g})$ gives $p_\theta(\mathbf{m}_{\mathcal{J}} | \mathbf{g})$, that by **D1** reduces to $p_\theta(\mathbf{m}_{\mathcal{J}} | \mathbf{g}_{\mathcal{I}})$, hence the term appearing in the third line. In the fourth line, we denoted with $p_{\lambda, \theta}(y) = \int q_\lambda(y | \mathbf{m}_{\mathcal{J}}) p_\theta(\mathbf{m}_{\mathcal{J}} | \mathbf{g}_{\mathcal{I}}) p(\mathbf{g}_{\mathcal{I}}) d\mathbf{m}_{\mathcal{J}} d\mathbf{g}_{\mathcal{I}}$ and reduced the first integral in $p(y)$. Finally, we obtain the upper bound for the first term of Λ , where the maximum implies having a vanishing KL term. Therefore, we have that:

$$\Lambda \leq 0 \tag{36}$$

Now, since Λ is lower bounded by the mutual information $I(\mathbf{M}_{\mathcal{J}}, Y)$, it cannot be negative and hence must be zero. This concludes the proof.

A.4 Proof of Corollay 1

The result of the corollary follows from proposition 3 by considering only the subset of representations $\mathbf{M}_{\mathcal{J}}$ that are not aligned to G_k . Denote them with $\mathbf{M}_{\mathcal{K}}$, where $\mathcal{K} = \{j : \pi(j) \neq k\}$ and set $\mathbf{G}_{-\mathcal{I}} = \mathbf{G}_{-\mathcal{I}} \cup G_k$. Then, we have:

$$p_\theta(\mathbf{m}_{\mathcal{K}} | \mathbf{g}) = p_\theta(\mathbf{m}_{\mathcal{K}} | \mathbf{g}_{\mathcal{I} \setminus \{g_k\}}) \tag{37}$$

Similarly to proposition 3, we then obtain that $\Lambda = 0$, *i.e.*, concept leakage vanishes. This proves the claim.

A.5 Proof of Proposition 4

For a given block $\mathbf{M}_{\mathcal{K}}$ aligned to $\mathbf{G}_{\Pi(\mathcal{K})}$, recall that by **D1** in definition 8 it holds that:

$$\mathbf{M}_{\mathcal{K}} = \mu_{\mathcal{K}}(\mathbf{G}_{\Pi(\mathcal{K})}, \mathbf{N}_{\mathcal{K}}) \tag{38}$$

To prove the first claim, we have to show that after intervening on $\mathbf{G}_{\Pi(\mathcal{K})}$ interventions on distinct $\mathbf{G}_{-\Pi(\mathcal{K})}$ do not affect $\mathbf{M}_{\mathcal{K}}$. Fix $do(\mathbf{G}_{\Pi(\mathcal{K})} \leftarrow \mathbf{g}_{\Pi(\mathcal{K})})$. Upon performing a second intervention on the remaining variables $do(\mathbf{G}_{-\Pi(\mathcal{K})} \leftarrow \mathbf{g}_{-\Pi(\mathcal{K})})$, we get:

$$p(\mathbf{G} | do(\mathbf{G}_{\Pi(\mathcal{K})} \leftarrow \mathbf{g}_{\Pi(\mathcal{K})}, \mathbf{G}_{-\Pi(\mathcal{K})} \leftarrow \mathbf{g}_{-\Pi(\mathcal{K})})) = \mathbb{1}\{(\mathbf{G}_{\Pi(\mathcal{K})}, \mathbf{G}_{-\Pi(\mathcal{K})}) = (\mathbf{g}_{\Pi(\mathcal{K})}, \mathbf{g}_{-\Pi(\mathcal{K})})\} \tag{39}$$

By **D1** of definition 8, it holds that the corresponding probability distribution on $\mathbf{M}_{\mathcal{K}}$ can be written as:

$$p(\mathbf{M}_{\mathcal{K}} | do(\mathbf{G}_{\Pi(\mathcal{K})} \leftarrow \mathbf{g}_{\Pi(\mathcal{K})})) = p(\mathbf{M}_{\mathcal{K}} | \mathbf{g}_{\Pi(\mathcal{K})}) \tag{40}$$

which by a similar argument to proposition 1 leads to a vanishing PIDA($\mathbf{G}_{\Pi(\mathcal{K})}, \mathbf{M}_{\mathcal{K}} | \mathbf{g}_{\Pi(\mathcal{K})}, \mathbf{g}_{-\Pi(\mathcal{K})}$), for all possible interventions $do(\mathbf{G}_{-\Pi(\mathcal{K})} \leftarrow \mathbf{g}_{-\Pi(\mathcal{K})})$. This proves that after intervening on $\mathbf{G}_{\Pi(\mathcal{K})}$, arbitrary interventions on $\mathbf{G}_{-\Pi(\mathcal{K})}$ do not affect $\mathbf{M}_{\mathcal{K}}$.

For the second claim, we consider two different intervened values $\mathbf{g}'_{\Pi(\mathcal{K})}$ and $\mathbf{g}''_{\Pi(\mathcal{K})}$ for $\mathbf{G}_{\Pi(\mathcal{K})}$. Recall that by **D2** in definition 8 it holds that the mean value of $\mathbf{M}_{\mathcal{K}}$ is connected to $\mathbf{G}_{\Pi(\mathcal{K})}$ by an invertible map. Therefore, it holds that:

$$\mathbf{g}'_{\Pi(\mathcal{K})} \neq \mathbf{g}''_{\Pi(\mathcal{K})} \implies \mathbb{E}_{\mathbf{N}_{\mathcal{K}}}[\mu_{\mathcal{K}}(\mathbf{g}'_{\Pi(\mathcal{K})}, \mathbf{N}_{\mathcal{K}})] \neq \mathbb{E}_{\mathbf{N}_{\mathcal{K}}}[\mu_{\mathcal{K}}(\mathbf{g}''_{\Pi(\mathcal{K})}, \mathbf{N}_{\mathcal{K}})] \tag{41}$$

by invertibility. This concludes the proof.

References

- Riccardo Guidotti, Anna Monreale, Salvatore Ruggieri, Franco Turini, Fosca Giannotti, and Dino Pedreschi. A survey of methods for explaining black box models. *ACM computing surveys (CSUR)*, 51(5):1–42, 2018.
- Erik Štrumbelj and Igor Kononenko. Explaining prediction models and individual predictions with feature contributions. *Knowledge and information systems*, 41(3):647–665, 2014.
- Marco Tulio Ribeiro, Sameer Singh, and Carlos Guestrin. “Why should I Trust You?” Explaining the predictions of any classifier. In *Proceedings of the 22nd ACM SIGKDD international conference on knowledge discovery and data mining*, pages 1135–1144, 2016.
- Been Kim, Rajiv Khanna, and Oluwasanmi O Koyejo. Examples are not enough, learn to criticize! criticism for interpretability. *Advances in neural information processing systems*, 29, 2016.
- Pang Wei Koh and Percy Liang. Understanding black-box predictions via influence functions. In *International conference on machine learning*, pages 1885–1894. PMLR, 2017.
- Berk Ustun and Cynthia Rudin. Supersparse linear integer models for optimized medical scoring systems. *Machine Learning*, 102(3):349–391, 2016.
- Tong Wang, Cynthia Rudin, Finale Doshi-Velez, Yimin Liu, Erica Klampfl, and Perry MacNeille. A bayesian framework for learning rule sets for interpretable classification. *The Journal of Machine Learning Research*, 18(1):2357–2393, 2017.
- Cynthia Rudin. Stop explaining black box machine learning models for high stakes decisions and use interpretable models instead. *Nature Machine Intelligence*, 1(5):206–215, 2019.
- Stefano Teso, Öznur Alkan, Wolfgang Stammer, and Elizabeth Daly. Leveraging explanations in interactive machine learning: An overview. *Frontiers in Artificial Intelligence*, 2023.
- Subbarao Kambhampati, Sarath Sreedharan, Mudit Verma, Yantian Zha, and Lin Guan. Symbols as a lingua franca for bridging human-ai chasm for explainable and advisable ai systems. In *Proceedings of the AAAI Conference on Artificial Intelligence*, volume 36, pages 12262–12267, 2022.
- Been Kim, Martin Wattenberg, Justin Gilmer, Carrie Cai, James Wexler, Fernanda Viegas, et al. Interpretability beyond Feature Attribution: Quantitative Testing with Concept Activation Vectors (TCAV). In *International conference on machine learning*, pages 2668–2677. PMLR, 2018.
- Ruth Fong and Andrea Vedaldi. Net2vec: Quantifying and explaining how concepts are encoded by filters in deep neural networks. In *Proceedings of the IEEE conference on computer vision and pattern recognition*, pages 8730–8738, 2018.
- Amirata Ghorbani, Abubakar Abid, and James Zou. Interpretation of neural networks is fragile. In *Proceedings of the AAAI Conference on Artificial Intelligence*, volume 33, pages 3681–3688, 2019.
- Ruihan Zhang, Prashan Madumal, Tim Miller, Krista A Ehinger, and Benjamin IP Rubinstein. Invertible concept-based explanations for cnn models with non-negative concept activation vectors. In *Proceedings of the AAAI Conference on Artificial Intelligence*, volume 35, pages 11682–11690, 2021.
- Thomas Fel, Agustin Picard, Louis Bethune, Thibaut Boissin, David Vigouroux, Julien Colin, Rémi Cadène, and Thomas Serre. Craft: Concept recursive activation factorization for explainability. In *Proceedings of the IEEE/CVF Conference on Computer Vision and Pattern Recognition*, pages 2711–2721, 2023a.
- David Alvarez-Melis and Tommi S Jaakkola. Towards robust interpretability with self-explaining neural networks. In *Proceedings of the 32nd International Conference on Neural Information Processing Systems*, pages 7786–7795, 2018.
- Chaofan Chen, Oscar Li, Daniel Tao, Alina Barnett, Cynthia Rudin, and Jonathan K Su. This looks like that: Deep learning for interpretable image recognition. *Advances in Neural Information Processing Systems*, 32:8930–8941, 2019.
- Pang Wei Koh, Thao Nguyen, Yew Siang Tang, Stephen Mussmann, Emma Pierson, Been Kim, and Percy Liang. Concept bottleneck models. In *International Conference on Machine Learning*, pages 5338–5348. PMLR, 2020.
- Emanuele Marconato, Andrea Passerini, and Stefano Teso. Glancenets: Interpretable, leak-proof concept-based models. In *NeurIPS*, 2022.

- Mateo Espinosa Zarlenga, Pietro Barbiero, Gabriele Ciravegna, Giuseppe Marra, Francesco Giannini, Michelangelo Diligenti, Zohreh Shams, Frederic Precioso, Stefano Melacci, Adrian Weller, Pietro Liò, and Mateja Jamnik. Concept embedding models. 2022.
- Zachary C Lipton. The mythos of model interpretability: In machine learning, the concept of interpretability is both important and slippery. *Queue*, 16(3):31–57, 2018.
- Gesina Schwalbe. Concept embedding analysis: A review. *arXiv preprint arXiv:2203.13909*, 2022.
- Wolfgang Stammer, Patrick Schramowski, and Kristian Kersting. Right for the Right Concept: Revising Neuro-Symbolic Concepts by Interacting with their Explanations. In *Proceedings of the IEEE/CVF Conference on Computer Vision and Pattern Recognition*, pages 3619–3629, 2021.
- Andrea Bontempelli, Stefano Teso, Fausto Giunchiglia, and Andrea Passerini. Concept-level debugging of part-prototype networks. In *International Conference on Learning Representations*, 2023.
- Adrian Hoffmann, Claudio Fanconi, Rahul Rade, and Jonas Kohler. This looks like that... does it? shortcomings of latent space prototype interpretability in deep networks. *arXiv preprint arXiv:2105.02968*, 2021.
- Romain Xu-Darme, Georges Quénot, Zakaria Chihani, and Marie-Christine Rousset. Sanity checks for patch visualisation in prototype-based image classification. In *Proceedings of the IEEE/CVF Conference on Computer Vision and Pattern Recognition*, pages 3690–3695, 2023.
- Zhi Chen, Yijie Bei, and Cynthia Rudin. Concept whitening for interpretable image recognition. *Nature Machine Intelligence*, 2(12):772–782, 2020.
- Andrei Margeloiu, Matthew Ashman, Umang Bhatt, Yanzhi Chen, Mateja Jamnik, and Adrian Weller. Do concept bottleneck models learn as intended? *arXiv preprint arXiv:2105.04289*, 2021.
- Anita Mahinpei, Justin Clark, Isaac Lage, Finale Doshi-Velez, and Weiwei Pan. Promises and pitfalls of black-box concept learning models. In *International Conference on Machine Learning: Workshop on Theoretic Foundation, Criticism, and Application Trend of Explainable AI*, volume 1, pages 1–13, 2021.
- Daniel L Silver and Tom M Mitchell. The roles of symbols in neural-based ai: They are not what you think! *arXiv preprint arXiv:2304.13626*, 2023.
- Bernhard Schölkopf, Francesco Locatello, Stefan Bauer, Nan Rosemary Ke, Nal Kalchbrenner, Anirudh Goyal, and Yoshua Bengio. Toward causal representation learning. *Proceedings of the IEEE*, 109(5): 612–634, 2021.
- Yoshua Bengio, Aaron Courville, and Pascal Vincent. Representation learning: A review and new perspectives. *IEEE transactions on pattern analysis and machine intelligence*, 35(8):1798–1828, 2013.
- Irina Higgins, David Amos, David Pfau, Sebastien Racaniere, Loic Matthey, Danilo Rezende, and Alexander Lerchner. Towards a definition of disentangled representations. *arXiv preprint arXiv:1812.02230*, 2018.
- Sander Beckers and Joseph Y Halpern. Abstracting causal models. In *Proceedings of the aaai conference on artificial intelligence*, volume 33, pages 2678–2685, 2019.
- Sander Beckers, Frederick Eberhardt, and Joseph Y Halpern. Approximate causal abstractions. In *Uncertainty in Artificial Intelligence*, pages 606–615. PMLR, 2020.
- Atticus Geiger, Zhengxuan Wu, Christopher Potts, Thomas Icard, and Noah D Goodman. Finding alignments between interpretable causal variables and distributed neural representations. *arXiv preprint arXiv:2303.02536*, 2023a.
- Joshua Lockhart, Nicolas Marchesotti, Daniele Magazzeni, and Manuela Veloso. Towards learning to explain with concept bottleneck models: mitigating information leakage. *arXiv preprint arXiv:2211.03656*, 2022.
- Judea Pearl. *Causality*. Cambridge university press, 2009.
- Jonas Peters, Dominik Janzing, and Bernhard Schölkopf. *Elements of causal inference: foundations and learning algorithms*. 2017.
- Cian Eastwood and Christopher KI Williams. A framework for the quantitative evaluation of disentangled representations. In *International Conference on Learning Representations*, 2018.

- Raphael Suter, Djordje Miladinovic, Bernhard Schölkopf, and Stefan Bauer. Robustly disentangled causal mechanisms: Validating deep representations for interventional robustness. In *International Conference on Machine Learning*, pages 6056–6065. PMLR, 2019.
- Abbavaram Gowtham Reddy, Vineeth N Balasubramanian, et al. On causally disentangled representations. In *Proceedings of the AAAI Conference on Artificial Intelligence*, volume 36, pages 8089–8097, 2022.
- Julius von Kügelgen, Yash Sharma, Luigi Gresele, Wieland Brendel, Bernhard Schölkopf, Michel Besserve, and Francesco Locatello. Self-supervised learning with data augmentations provably isolates content from style. In *Proceedings of the 35nd International Conference on Neural Information Processing Systems*, 2021.
- Daphne Koller and Nir Friedman. *Probabilistic graphical models: principles and techniques*. MIT press, 2009.
- Andrea Bontempelli, Fausto Giunchiglia, Andrea Passerini, and Stefano Teso. Toward a Unified Framework for Debugging Gray-box Models. In *The AAAI-22 Workshop on Interactive Machine Learning*, 2021.
- Mateo Espinosa Zarlenga, Barbiero Pietro, Ciravegna Gabriele, Marra Giuseppe, Francesco Giannini, Michelangelo Diligenti, Shams Zohreh, Precioso Frederic, Stefano Melacci, Weller Adrian, et al. Concept embedding models: Beyond the accuracy-explainability trade-off. In *Advances in Neural Information Processing Systems*, volume 35, pages 21400–21413. Curran Associates, Inc., 2022.
- Thomas Fel, Victor Boutin, Mazda Moayeri, Rémi Cadène, Louis Bethune, Léo andéol, Mathieu Chalvidal, and Thomas Serre. A holistic approach to unifying automatic concept extraction and concept importance estimation, 2023b.
- Stefano Teso. Toward faithful explanatory active learning with self-explainable neural nets. In *Proceedings of the Workshop on Interactive Adaptive Learning (IAL 2019)*, pages 4–16, 2019.
- Jacob Pfau, Albert T Young, Jerome Wei, Maria L Wei, and Michael J Keiser. Robust semantic interpretability: Revisiting concept activation vectors. *arXiv preprint arXiv:2104.02768*, 2021.
- Aviv Gabbay, Niv Cohen, and Yedid Hoshen. An image is worth more than a thousand words: Towards disentanglement in the wild. *Advances in Neural Information Processing Systems*, 34, 2021.
- Loic Matthey, Irina Higgins, Demis Hassabis, and Alexander Lerchner. dsprites: Disentanglement testing sprites dataset. <https://github.com/deepmind/dsprites-dataset/>, 2017.
- Marton Havasi, Sonali Parbhoo, and Finale Doshi-Velez. Addressing leakage in concept bottleneck models. 2022.
- Thomas M Cover. *Elements of information theory*. John Wiley & Sons, 1999.
- Milton Llera Montero, Casimir JH Ludwig, Rui Ponte Costa, Gaurav Malhotra, and Jeffrey Bowers. The role of disentanglement in generalisation. In *International Conference on Learning Representations*, 2020.
- Milton Montero, Jeffrey Bowers, Rui Ponte Costa, Casimir Ludwig, and Gaurav Malhotra. Lost in latent space: Examining failures of disentangled models at combinatorial generalisation. *Advances in Neural Information Processing Systems*, 35:10136–10149, 2022.
- Xin Sun, Zhenning Yang, Chi Zhang, Keck-Voon Ling, and Guohao Peng. Conditional gaussian distribution learning for open set recognition. In *Proceedings of the IEEE/CVF Conference on Computer Vision and Pattern Recognition*, pages 13480–13489, 2020.
- Aapo Hyvarinen and Hiroshi Morioka. Nonlinear ica of temporally dependent stationary sources. In *Artificial Intelligence and Statistics*, pages 460–469. PMLR, 2017.
- Ilyes Khemakhem, Ricardo Pio Monti, Diederik P. Kingma, and Aapo Hyvärinen. Ice-beem: Identifiable conditional energy-based deep models based on nonlinear ica, 2020a.
- Paul K Rubenstein, Sebastian Weichwald, Stephan Bongers, Joris M Mooij, Dominik Janzing, Moritz Grosse-Wentrup, and Bernhard Schölkopf. Causal consistency of structural equation models. *arXiv preprint arXiv:1707.00819*, 2017.
- Fabio Massimo Zennaro. Abstraction between structural causal models: A review of definitions and properties. *arXiv preprint arXiv:2207.08603*, 2022.
- Atticus Geiger, Chris Potts, and Thomas Icard. Causal abstraction for faithful model interpretation. *arXiv preprint arXiv:2301.04709*, 2023b.

- Louis Marti, Shengyi Wu, Steven T Piantadosi, and Celeste Kidd. Latent diversity in human concepts. *Open Mind*, 7:79–92, 2023.
- Julian Zaidi, Jonathan Boilard, Ghyslain Gagnon, and Marc-André Carbonneau. Measuring disentanglement: A review of metrics. *arXiv preprint arXiv:2012.09276*, 2020.
- Cian Eastwood, Andrei Liviu Nicolicioiu, Julius Von Kügelgen, Armin Kekić, Frederik Träuble, Andrea Dittadi, and Bernhard Schölkopf. Dci-es: An extended disentanglement framework with connections to identifiability. *arXiv preprint arXiv:2210.00364*, 2022.
- Ricky TQ Chen, Xuechen Li, Roger Grosse, and David Duvenaud. Isolating sources of disentanglement in vaes. In *Proceedings of the 32nd International Conference on Neural Information Processing Systems*, pages 2615–2625, 2018.
- Francesco Locatello, Stefan Bauer, Mario Lucic, Gunnar Raetsch, Sylvain Gelly, Bernhard Schölkopf, and Olivier Bachem. Challenging common assumptions in the unsupervised learning of disentangled representations. In *International Conference on Machine Learning*, pages 4114–4124, 2019.
- Tuomas Oikarinen, Subhro Das, Lam M Nguyen, and Tsui-Wei Weng. Label-free concept bottleneck models. In *ICLR*, 2022.
- Isaac Lage and Finale Doshi-Velez. Learning interpretable concept-based models with human feedback. *arXiv preprint arXiv:2012.02898*, 2020.
- Kushal Chauhan, Rishabh Tiwari, Jan Freyberg, Pradeep Shenoy, and Krishnamurthy Dvijotham. Interactive concept bottleneck models. In *AAAI*, 2023.
- Stephen Muggleton and Luc De Raedt. Inductive logic programming: Theory and methods. *The Journal of Logic Programming*, 19:629–679, 1994.
- Luc De Raedt, Sebastijan Dumancic, Robin Manhaeve, and Giuseppe Marra. From statistical relational to neuro-symbolic artificial intelligence. In *IJCAI*, 2020.
- Ilyes Khemakhem, Diederik Kingma, Ricardo Monti, and Aapo Hyvarinen. Variational autoencoders and nonlinear ica: A unifying framework. In *International Conference on Artificial Intelligence and Statistics*, pages 2207–2217. PMLR, 2020b.
- Mara Graziani, An-phi Nguyen, Laura O’Mahony, Henning Müller, and Vincent Andrearczyk. Concept discovery and dataset exploration with singular value decomposition. In *ICLR 2023 Workshop on Pitfalls of limited data and computation for Trustworthy ML*, 2023.
- Oscar Li, Hao Liu, Chaofan Chen, and Cynthia Rudin. Deep learning for case-based reasoning through prototypes: A neural network that explains its predictions. In *Proceedings of the AAAI Conference on Artificial Intelligence*, 2018.
- Dawid Rymarczyk, Łukasz Struski, Jacek Tabor, and Bartosz Zieliński. ProtoPShare: Prototypical Parts Sharing for Similarity Discovery in Interpretable Image Classification. In *Proceedings of the 27th ACM SIGKDD Conference on Knowledge Discovery & Data Mining*, page 1420–1430, 2021.
- Meike Nauta, Ron van Bree, and Christin Seifert. Neural prototype trees for interpretable fine-grained image recognition. In *Proceedings of the IEEE/CVF Conference on Computer Vision and Pattern Recognition*, pages 14933–14943, 2021.
- Gurmail Singh and Kin-Choong Yow. These do not look like those: An interpretable deep learning model for image recognition. *IEEE Access*, 9:41482–41493, 2021.
- Seyed Omid Davoudi and Majid Komeili. Toward faithful case-based reasoning through learning prototypes in a nearest neighbor-friendly space. In *International Conference on Learning Representations*, 2021.
- Bolei Zhou, Yiyou Sun, David Bau, and Antonio Torralba. Interpretable basis decomposition for visual explanation. In *Proceedings of the European Conference on Computer Vision (ECCV)*, pages 119–134, 2018.
- Dmitry Kazhdan, Boty Dimanov, Mateja Jamnik, Pietro Liò, and Adrian Weller. Now you see me (cme): concept-based model extraction. *arXiv preprint arXiv:2010.13233*, 2020.
- Jindong Gu and Volker Tresp. Semantics for global and local interpretation of deep neural networks. *arXiv preprint arXiv:1910.09085*, 2019.
- Patrick Esser, Robin Rombach, and Bjorn Ommer. A disentangling invertible interpretation network for explaining latent representations. In *Proceedings of the IEEE/CVF Conference on Computer Vision and Pattern Recognition*, pages 9223–9232, 2020.

- Mert Yuksekgonul, Maggie Wang, and James Zou. Post-hoc concept bottleneck models. *arXiv preprint arXiv:2205.15480*, 2022.
- Yoshihide Sawada and Keigo Nakamura. Concept bottleneck model with additional unsupervised concepts. *IEEE Access*, 2022.
- Luca Erculiani, Andrea Bontempelli, Andrea Passerini, and Fausto Giunchiglia. Egocentric hierarchical visual semantics. *arXiv preprint arXiv:2305.05422*, 2023.
- Irina Higgins, Loic Matthey, Arka Pal, Christopher Burgess, Xavier Glorot, Matthew Botvinick, Shakir Mohamed, and Alexander Lerchner. β -vae: Learning basic visual concepts with a constrained variational framework. In *International Conference on Learning Representations*, 2016.
- Diederik P Kingma and Max Welling. Auto-encoding variational bayes. In *International conference on machine learning*. PMLR, 2014.
- Hyunjik Kim and Andriy Mnih. Disentangling by factorising. In *International Conference on Machine Learning*, pages 2649–2658. PMLR, 2018.
- Babak Esmaeili, Hao Wu, Sarthak Jain, Alican Bozkurt, Narayanaswamy Siddharth, Brooks Paige, Dana H Brooks, Jennifer Dy, and Jan-Willem Meent. Structured disentangled representations. In *The 22nd International Conference on Artificial Intelligence and Statistics*, pages 2525–2534. PMLR, 2019.
- Travers Rhodes and Daniel Lee. Local disentanglement in variational auto-encoders using jacobian l_1 regularization. *Advances in Neural Information Processing Systems*, 34:22708–22719, 2021.
- Francesco Locatello, Michael Tschannen, Stefan Bauer, Gunnar Rätsch, Bernhard Schölkopf, and Olivier Bachem. Disentangling factors of variations using few labels. In *International Conference on Learning Representations*, 2020a.
- Rui Shu, Yining Chen, Abhishek Kumar, Stefano Ermon, and Ben Poole. Weakly supervised disentanglement with guarantees. In *International Conference on Learning Representations*, 2020.
- Francesco Locatello, Ben Poole, Gunnar Rätsch, Bernhard Schölkopf, Olivier Bachem, and Michael Tschannen. Weakly-supervised disentanglement without compromises. In *International Conference on Machine Learning*, pages 6348–6359. PMLR, 2020b.
- Sébastien Lachapelle, Pau Rodriguez, Yash Sharma, Katie E Everett, Rémi Le Priol, Alexandre Lacoste, and Simon Lacoste-Julien. Disentanglement via mechanism sparsity regularization: A new principle for nonlinear ica. In *Conference on Causal Learning and Reasoning*, pages 428–484. PMLR, 2022.
- Daniella Horan, Eitan Richardson, and Yair Weiss. When is unsupervised disentanglement possible? *Advances in Neural Information Processing Systems*, 34, 2021.
- Wolfgang Stammer, Marius Memmel, Patrick Schramowski, and Kristian Kersting. Interactive disentanglement: Learning concepts by interacting with their prototype representations. In *Proceedings of the IEEE/CVF Conference on Computer Vision and Pattern Recognition*, pages 10317–10328, 2022.
- Pierre Comon. Independent component analysis, a new concept? *Signal processing*, 36(3):287–314, 1994.
- Aapo Hyvärinen, Juha Karhunen, and Erkki Oja. Independent component analysis, adaptive and learning systems for signal processing, communications, and control. *John Wiley & Sons, Inc*, 1:11–14, 2001.
- Ganesh R Naik and Dinesh K Kumar. An overview of independent component analysis and its applications. *Informatica*, 35(1), 2011.
- Aapo Hyvärinen and Petteri Pajunen. Nonlinear independent component analysis: Existence and uniqueness results. *Neural networks*, 12(3):429–439, 1999.
- Simon Buchholz, Michel Besserve, and Bernhard Schölkopf. Function classes for identifiable nonlinear independent component analysis. *Advances in Neural Information Processing Systems*, 35:16946–16961, 2022.
- Chih-Kuan Yeh, Been Kim, Sercan Arik, Chun-Liang Li, Tomas Pfister, and Pradeep Ravikumar. On completeness-aware concept-based explanations in deep neural networks. *Advances in neural information processing systems*, 33:20554–20565, 2020.
- Mateo Espinosa Zarlenga, Pietro Barbiero, Zohreh Shams, Dmitry Kazhdan, Umang Bhatt, Adrian Weller, and Mateja Jamnik. Towards robust metrics for concept representation evaluation, 2023.

- Robin Manhaeve, Sebastijan Dumancic, Angelika Kimmig, Thomas Demeester, and Luc De Raedt. DeepProbLog: Neural Probabilistic Logic Programming. *NeurIPS*, 2018.
- Ivan Donadello, Luciano Serafini, and Artur D’Avila Garcez. Logic tensor networks for semantic image interpretation. *arXiv preprint arXiv:1705.08968*, 2017.
- Michelangelo Diligenti, Marco Gori, and Claudio Sacca. Semantic-based regularization for learning and inference. *Artificial Intelligence*, 244:143–165, 2017.
- Marc Fischer, Mislav Balunovic, Dana Drachler-Cohen, Timon Gehr, Ce Zhang, and Martin Vechev. DL2: Training and querying neural networks with logic. In *International Conference on Machine Learning*, pages 1931–1941. PMLR, 2019.
- Eleonora Giunchiglia and Thomas Lukasiewicz. Coherent hierarchical multi-label classification networks. *NeurIPS*, 2020.
- Zhun Yang, Adam Ishay, and Joohyung Lee. NeurASP: Embracing neural networks into answer set programming. In *IJCAI*, 2020.
- Jiani Huang, Ziyang Li, Binghong Chen, Karan Samel, Mayur Naik, Le Song, and Xujie Si. Scallop: From probabilistic deductive databases to scalable differentiable reasoning. *NeurIPS*, 2021.
- Giuseppe Marra and Ondřej Kuželka. Neural markov logic networks. In *Uncertainty in Artificial Intelligence*, 2021.
- Kareem Ahmed, Stefano Teso, Kai-Wei Chang, Guy Van den Broeck, and Antonio Vergari. Semantic Probabilistic Layers for Neuro-Symbolic Learning. In *NeurIPS*, 2022.
- Eleonora Misino, Giuseppe Marra, and Emanuele Sansone. VAEL: Bridging Variational Autoencoders and Probabilistic Logic Programming. *NeurIPS*, 2022.
- Thomas Winters, Giuseppe Marra, Robin Manhaeve, and Luc De Raedt. DeepStochLog: Neural Stochastic Logic Programming. In *AAAI*, 2022.
- Emile van Krieken, Thiviyan Thanapalasingam, Jakub M Tomczak, Frank van Harmelen, and Annette ten Teije. A-nesi: A scalable approximate method for probabilistic neurosymbolic inference. *arXiv preprint arXiv:2212.12393*, 2022.
- Gabriele Ciravegna, Pietro Barbiero, Francesco Giannini, Marco Gori, Pietro Lió, Marco Maggini, and Stefano Melacci. Logic explained networks. *Artificial Intelligence*, 314:103822, 2023.
- Emanuele Marconato, Gianpaolo Bontempo, Elisa Ficarra, Simone Calderara, Andrea Passerini, and Stefano Teso. Neuro symbolic continual learning: Knowledge, reasoning shortcuts and concept rehearsal. In *ICML*, 2023a.
- Emanuele Marconato, Stefano Teso, Antonio Vergari, and Andrea Passerini. Not all neuro-symbolic concepts are created equal: Analysis and mitigation of reasoning shortcuts. *arXiv preprint arXiv:2305.19951*, 2023b.